IDM UID
222QGL
VERSION CREATED ON / VERSION / STATUS
09 Jan 2017 / 6.2 / Approved
EXTERNAL REFERENCE / VERSION

Guideline

Load Specifications (LS)

This document contains the ITER project-level technical requirements related to load specification to be used for all systems of the ITER machine.

Approval Process			
	Name	*Action*	*Affiliation*
Signatory	**Sannazzaro G.**	**09 Jan 2017:signed**	**IO/DG/COO/CIO/AS**
Co-signatories			
Reviewers	**Alekseev A.** **Janeschitz G.**	**09 Jan 2017:recommended (Fast Track)** **23 Jan 2017:recommended**	**IO/DG/COO/TED** **IO/DG/COO/CIO**
Previous Versions Reviews	**Elbez-Uzan J.** **Campbell D.** **Bak J.- S.** **Chiocchio S.** **Onozuka M.** **Zhao Z.**	**12 Dec 2016:recommended v6.1** **20 Dec 2016:recommended v6.1** **05 Dec 2016:recommended v6.1** **19 Dec 2016:recommended v6.1** **28 Nov 2016:recommended v6.1** **03 Jan 2017:recommended v6.1**	**IO/DG/RCO/SD/EPNS** **IO/DG/COO/SCOD** **IO/DG/COO/CST** **IO/DG/COO/CIO/CMD** **IO/DG/COO/CIO** **IO/DG/RCO/QAA**
Approver	**Lee G.- S.**	**23 Jan 2017:approved**	**IO/DG/COO**
Document Security: Internal Use *RO: Chiocchio Stefano*			
Read Access	**GG: MAC Members and Experts, GG: STAC Members & Experts, AD: ITER, AD: External Collaborators, AD: IO_Director-General, AD: EMAB, AD: Auditors, AD: ITER Management Assessor, project administrator, RO, LG: WG-5 Write Access, LG: Tech Spec Editorial Team, AD: OBS - Analysis Section Division (AS), GG: ...**		

Change Log			
Load Specifications (LS) (222QGL)			
Version	***Latest Status***	***Issue Date***	***Description of Change***
v1.0	Approved	22 Dec 2004	
v2.0	Approved	09 Feb 2005	
v3.0	Approved	08 Jul 2005	
v3.1	Approved	28 Apr 2006	
v3.2	Signed	28 Oct 2008	
v3.3	Signed	06 Jul 2009	The major changes come from the outcome of the STAC issues studies and the meeting with ASN/IRSN (French Regulatory Body). The numbers of VDE II, disruption I, and II to be considered for the design of the ITER components have been revised. - More precise definition of the cryostat and VV Ingress of Coolant Events (ICE), cryostat and VV loss of vacuum events, ex-cryostat coolant leakage events, VV loss of coolant events, magnets faults events, loss of power events to match defition in the Accident Analysis Report (AAR). - Paragraph 5.1 seismic requirement modified to separate definition of requirement for nuclear and non-nuclear buildings and equipment. - More detailed specifications of the seismic requirements - Seismic requirements defined consistent with the building seismic classification (SCI, SCII, and NSC). – Definition of SL-0 following Eurocode. - The maximum halo current for slow downward VDE is defined by the formula TPF*Ih/Ip=0.75 - An uncertainty factor of 1.2 on the computer simulation of halo current in VDEs and on machine experimental observation is introduced to include uncertainties. - Revision of the maximum VV loads following the final decisions of the STAC issues meeting defined in the TWG10 final reports - Definition of LOCA and LOFA and number of LOFA cat II events - Magnets faults event definition: The definition of these events has been removed, because it involves only the magnets system and not other componets. The definition of the magnets faults conditions and loads will be defined in a specific technical document - Included the definition of MD IV with faster current quench (26 ms for linear and 11.3 ms time constant for exponential decays respectively) Definition of VDE IV event with plasma in kink mode rotating at the natural frequency of the structure
v3.4	Signed	31 Jul 2009	In this version all comments received from the reviewers of the version 3.3 have been included. In addition the recommendations from PCR-175 have been implemented.
v3.5	Approved	10 Sep 2009	This new version has been issued to include the possibility of associating, for investment protection criteria or operational cost/time, category III and IV events with damage limits that are more stringent than those required by safety reasons (modification of table 2-2). Table 3-2 has also been improved to include accident conditions specified in AAR documents. The definition of the magnet fast discharge events have been improved providing more details and distinguishing between PF and CS current discharge and all magnet discharge events. The change mark-up file is in IDM attachment.
v4.0	Signed	16 Dec 2011	New version is uploaded following PCR 397
v5.0	Disapproved	23 Feb 2012	All comments to previous version 4.0 have been addressed and solved in this

			new version. The implemented changes can be seen opening the word file in the IDM attachment viewing it in track change mode. The main changes are: 5.0 2.0 Definition of category V event is introduced 3.0 Table 3-2 LOFA II and IV are removed from the list LOCA in Vault added to the list Several combinations between plasma transient events VV ICEs, MFDs and Cr ICEs have been included following the request of ITER Licencing Cell to be consistent with load case combinations presented to the French Regulator. Table 3-4 list of events in category V to be considered for the second safety confinement barrier. 4.6 Cr ICE of water is eliminated as it is prevented by guard pipes 5.1 Specification on the seismic requirement during initial machine assembly or installation are provided.

			5.1.1 Definition of scaling factor between SMHV and SL-2 soil spectra. SL-2 and SMHV spectra value defined at 0.5% of damping (used for liquids). The number of SL-1 events to be considered is 5 if required by investment protection. 5.1.1.3 Damping values for SMHV are “specified” and not “recommended” 5.1.2 Added Specification for seismic analysis of equipment inside the building Definition of coupled and decoupled equipment and associated analysis procedures. Added analysis method for liquids. 5.2 Slow_fast plasma current quench in disruption is defined only for category IV events Rotating asymmetric plasma are defined only for category IV event.

			5.2 and Appendix II Damping values for structural transient analysis of plasma transient events are defined in agreement with VV LS document. 5.3 Slow_fast plasma current quench in VDEs is defined only for category IV events 5.6 Table 5-19: value of maximum pressure in Cr ICE II is corrected 30 kPa instead of 300 kPa. 6.0 Modified references 27, 28, 29, 30. Ref 42- 47 introduced. Text in the document changed accordingly Appendix A Modified to reflect change in the main text

			Appendix II New appendix to provide specification for damping values for structural simulation of the tokamak components in plasma transient events
v6.0	Approved	20 Apr 2012	Version Chapter Changes 6.0 Formatting of document following ITER standards (see comments from JP Croset and D Sands). Chapter with purpose and scope are introduced and all chapter numbers are changed accordingly. Figures and tables numbers are changed accordingly. 5 Section 3 in previous version: Load combination: requests to include new combinations have been implemented. Table 5-2 and 5-4 have been modified accordingly. This responds to the IDM comments from C Alejaldre and L Patisson. 6 Section 4 in previous version: description of the machine support system has been changed following design modification of the cryostat supports.

			8 Section 6 in previous version: Unnecessary references have been removed. Other references (old or obsolete) have been replaced by more recent documents. Appendix B Modifications have been implemented in consistency with changes in table 5-2.
v6.1	Signed	17 Nov 2016	Implementation of minor PCR M365 (Implement ASN prescription on 700MW/100s fusion power and 17 MA plasma current into ITER baseline documents) with clarification of requirements for 700 MW fusion power and 17 MA plasma current requirements. Implementation of PCR 744 (Implementation of Construction Design Tokamak Complex FRS) for the update of Floor Response Spectra (FRS) from Tender Design (TD) and information about the need to perform reconciliation of calculation or design based on the as-built FRS. Included the warning that FRS for Hot Cell, Rad Waste and Personnel Control Access Buildings are based on a preliminary evaluation and will need to be updated following the design evolution. Correction of table B-1 and B-3 for consistency with the main text. Removal of typos and improvement of text for better clarification. All implemented changes can be found in the document in attachment.
v6.2	Approved	09 Jan 2017	In section 7.2 the duration of the burn time for the 500 MW nuclear fusion power in the inductive operational scenario is changed to 450 s instead of 400 s as specified in PR.

Table of Contents

1 Purpose

This document is an annex of the ITER project Requirement document [1] and provides a general description and definition of the main loads affecting the ITER machine and is mainly focused on the tokamak components.

The main purposes of this Load Specifications are:

- to describe the main loads affecting the tokamak and their load path through the mechanical connections;
- to specify the primary loading conditions which affect concurrently multiple tokamak components;
- to classify the loads and their combinations into the categories.

This document might not be sufficient to provide a fully comprehensive detail load specification on single systems or components, but provides the basis for the preparation of these types of technical specifications. These detail specifications are provided by documents that are herein called System Load Specification Documents or are provided by SRD.

2 Scope

This document contains the ITER project-level technical requirements related to load specification to be used for all systems of the ITER machine. The technical requirements specified in this document flow down to ITER systems for inclusion in System Requirements Documents (SRDs).

The definition of the heat loads from the plasma to the plasma facing components is outside the scope of this document. Heat and nuclear loads from the plasma are defined in [2].

3 Definitions

The ITER Active Web Abbreviations Dictionary can be found at the following URL:

https://portal.iter.org/Pages/abbreviations.aspx

A list of abbreviations is also reported in section 5 of PR Document [1].

Additional or more frequently used abbreviations are here reported.

AAR	Accident Analysis Report
ASCE	American Society of Civil Engineers
ASME	American Society of Mechanical Engineers
BLK	Blanket
CC	Correction Coil
CD	Central Disruption
CQ	Current Quench
CS	Central Solenoid
DDD	Design Description Document
DOF	Degree Of Freedom
DRS	Design Response Spectra
EM	Electro Magnetic
EOB	End Of Burn

FRS	Floor Response Spectra
FW	First Wall
ICE	Ingress of Coolant Event
Ihalo	Halo current
Ip	Plasma current
LOCA	Loss of Coolant Accident
LOFA	Loss of (forced) Flow Accident
LOOP	Loss Of Off-site Power
LOVA	Loss of Vacuum Accident
MD	Major Disruption
MFD	Magnet Fast (current) Discharge
MFD-I	Fast current discharge of PF and CS coils
MFD-II	Fast current discharge of all superconducting coil systems
MQP	Management Quality Program
NRC	Nuclear Regulatory Commission
NSC	Non-Seismic Class
PF	Poloidal Field
PFC	Poloidal Field Coil
PHTS	Primary heat Transport System
PR	Project Requirement (Document)
PRS	Point Response Spectra - Spectra calculated at specific points of a structure (also called "In-Structure Spectra" and "Secondary Spectra
RE	Runaway Electron
RPrS	Preliminary Safety Report (Rapport Préliminaire de Sûreté)
SC	Seismic Class
SIC	Safety Importance Class
SL	Seismic Level
SL-1	Seismic Level 1 – Defined by ITER for investment protection
SL-2	Seismic Level 2 – equivalent to Safe Shutdown Earthquake
SMHV	Séismes Maximaux Historiquement Vraisemblables = Maximum Historically Probable Earthquake
SOF	Start Of Flat top
SRD	System Requirement Document
SRSS	Square Root of Sum of Square
SSC	System, Structure, and Component
SSE	Safe Shutdown Earthquake
TF	Toroidal Field
TFC	Toroidal Field Coils
TPF	Toroidal Peaking factor
TQ	Thermal Quench
VDE	Vertical Displacement Event

VV	Vacuum Vessel
VVPSS	Vacuum Vessel Pressure Suppression System
ZPA	Zero Period Acceleration

4 Loads categories

The ITER loading conditions are categorized, into four classes based on the expectation of occurrence:

Category I: Operational Loading Conditions
Category II: Likely Loading Conditions
Category III: Unlikely Loading Conditions
Category IV: Extremely Unlikely Loading Conditions

Other events or events combinations that are beyond design basis may be classified in an additional category (category V). Unless specifically required by safety or project decision, the events in this category do not need to be considered for the design of the mechanical components, but they may be required for the secondary safety barrier.

The typical process of component design involves the following steps:

1) Identify and specify all conditions (e.g., Seismic, Gravity, Disruptions, etc.);
2) Identify and categorize condition combinations (e.g., Seismic + Disruption);
   - Evaluate loads arising from each condition combination;
   - Calculate the stresses due to each load combination;
3) Establish the acceptable damage limit for each condition combination (e.g., Normal, Upset, Emergency, or Faulted) also based on whether the component has any safety importance. Details can be found in PR [1];
4) Establish the structural service criteria for each damage limit (e.g., ASME Level A, B, C, and D). The structural service criteria are defined in the design code selected for the component (definition of the selected C&S for each system is defined in [47]);
5) Compare the evaluated stresses against the established criteria.

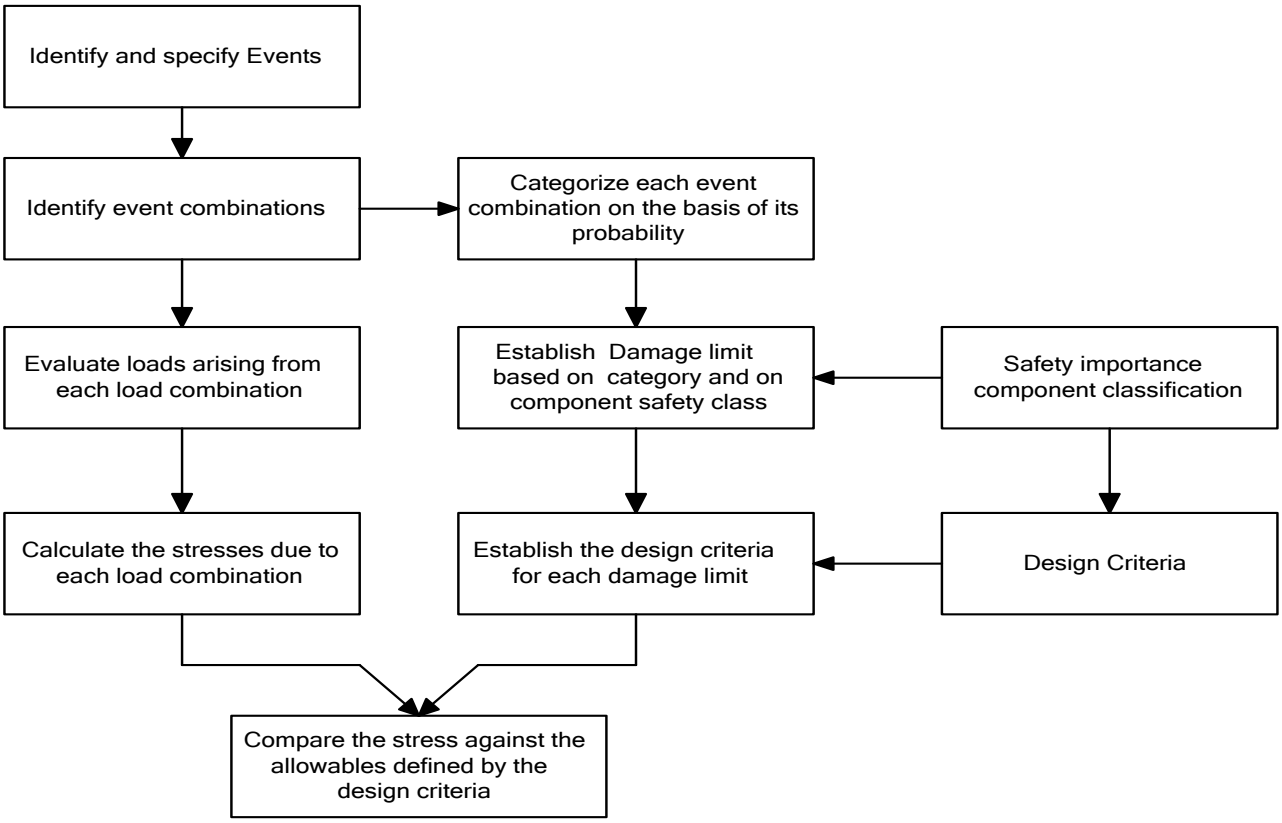

Figure 4-1 Flow Diagram of Typical Design and Assessment Process

The following table indicates the definition of different types of damage limits for components and plant.

Table 4-1: Damage Limits in Plant and Component Level

Condition	Damage Limits to Component Level	Damage Limits in Plant Level and Recovery of the Plant (Plant Operational Condition)
Normal/ Design/ test	The component should maintain specified service function.	Within specified operational limit. No special inspection will be required other than routine maintenance and minor adjustment. For test condition inspections are required as specified in the selected C&S
Upset	The component must withstand these loadings without significant damage requiring special inspection or repair.	After minor adjustment, or replacement of the faulty component, the plant can be brought back to normal operation. No effect on other components that may call for special inspection or repair.
Emergency	Large deformations in areas of structural discontinuity, such as at nozzles, which may necessitate removal of the component from service for inspection or repair. Insignificant general permanent deformation that may affect safety function of the component concerned. General strains should be within elastic limits. Active components should be functional at least after transient.	The plant may require decontamination, major replacement of damaged component or major repair work. In addition to the damaged component, inspection may reveal localised large deformation in other components, which may call for the repair of the affected components. Nevertheless, the plant maintains the specified minimum safety function during and after the events.
Faulted	Gross general deformations with some consequent loss of dimensional stability and damage requiring repair, which may require removal of component from service. Nevertheless deformation should not lead to structural collapse which could damage other components. The fluid boundary is maintained but degraded; however the safety function is maintained. The confinement of radioactive material is maintained. Active components may not be functional after transient.	Gross damage to the affected system or component. No loss of safety function which could lead to releases in excess of the guidelines established for Accidents. No design consideration will be given for recovery. The recovery of the plant may be judged from the severity of damage. This level of state is not expected to occur, but is postulated for safety assessment because its consequences would include the potential for the release of significant amounts of radioactive material.

The following table indicates the relationship between Load Combination Category (loads and likelihood categories) and acceptable damage limit as a function of the component safety class (SIC or non-SIC) [31].

The selected C&S defines the service level or service criteria (allowable value) to satisfy the damage limits.

Table 4-2: Damage Limits for Loading Condition Categories

Loading Category		Category I: Operational/ Design Loading	Category II: Likely Loading	Category III: Unlikely Loading	Category IV: Extremely Unlikely Loading	Test Loading
Plant Level		Normal	Normal	Emergency	Faulted	Normal/test
Component	SIC-1	Normal	Normal (4)	Emergency (3)	Faulted (1), (3)	Normal/test
	SIC-2 (5)	Normal	Normal (4)	Emergency (3)	Faulted (3)	Normal/test
	Non-SIC	Normal	Upset (3)	Emergency (2), (3)	Faulted (2), (3)	Normal/test

Notes

(1) Faulted for passive components with no deformation limits. Emergency for active SIC-1 components and some passive components in which general deformations should be limited.

(2) Events need not to be considered from the safety point of view, but only for investment protection if required.

(3) Damage limits can be made more stringent either for investment protection reasons or to reduce delay/cost of post incident inspections, for components where the design is sufficiently robust. Normal for some SIC-1 active components and some passive ones which are required to function following Category III and IV accident (e.g. fire dampers and detritiation system)

(4) Normal damage limits are assumed to have a robust design for SIC components not only for category I event, but also for category II.

(5) Damage limits can be modified based on case by case considerations (systems classified as SIC-2 are not credited for bringing the plant into a safe status)

5 Load combinations

A set of rules are being used across the ITER design to establish event combinations and to classify them. A fundamental question is to establish the probability of one condition triggering another loading event. In fact, after an initiating condition, other additional conditions may occur.

- Conditions are here called “probable” to occur if their conditional probability is higher than 1%.
- Conditions are here called “conceivable” to occur if their conditional probability is smaller than 1% but still plausible with some physical basis.

The 1% value is chosen based on the normal practise applied in nuclear power plants where the ratio between the probabilities of occurrence of two subsequent categories is of the order 10^{-2}.

Whenever lacking a more comprehensive probabilistic analysis, conditions are categorized as follows:

- Category I, for a combination of:
  - All Category I conditions when occurring at the same time or *"Probable"* to be triggered by the initiating condition.
- Category II, for a combination of:
  - The above Category I combinations with other Category I conditions also when they are "Conceivable" to be triggered by the initiating condition.
  - A Category II condition with other Category I and II conditions which are present or "Probable" to be triggered by the initiating condition.

- Category III, for a combination of:
    - The above Category II combinations with other Category II or I conditions also when they are "Conceivable" to be triggered by the initiating condition.
    - A Category III condition with other Category I, II, and III conditions which are present or "Probable" to be triggered by the initiating condition.
- Category IV, for a combination of:
    - The above Category III combinations with other Category III, or II or I conditions also when they are "Conceivable" to be triggered by the initiating condition.
    - A Category IV condition with other Category I, II, III, and IV conditions which are present or "Probable" to be triggered by the initiating condition.

A Category IV condition with any other event that is considered “Conceivable” to be triggered by the initiating condition is not considered in the design basis.

Following the above general considerations, Table 5-1 shows typical combinations. When multiple events are combined the overall likelihood of the combination has to be assessed to properly categorise it. The component designers have to identify the additional loads (gravity, pressure, thermal, etc.) that need to be considered for the related component. In Appendix B a full list of all single events and load case combinations is provided as a guideline (template) for the preparation of specific system load specifications.

See sections 7.1 for the definition of seismic events SL-1, SMHV, and SL-2. See section 6.3 and 7.2 for the definition of plasma disruptions MD I, II, III, and IV and vertical displacement events VDE II, III, and IV. See section 6.3.3 for the definition of the magnet fast discharge events MFD I and MFD II.

Ingress of coolant events (ICE) for vacuum vessel (VV) or Cryostat (Cr) are defined in 6.5 and 6.6.

Loss of vacuum accidents (LOVA) for VV and cryostat are defined in 6.7 and 6.8.

The Loss of Coolant Accidents (LOCA) outside the cryostat are defined in 6.9.

The VV Loss of forced flow accidents (VV LOFA) and loss of coolant accidents (VV LOCA) are defined in 6.10.

For the concatenation of events with fast plasma transients, it is assumed that the machine has a Disruption Mitigation System (DMS). The DMS initiates plasma disruption to:

- reduce the plasma kinetic energy just before the energy quench by the enhanced radiation;
- reduce the halo current and its toroidal peaking by forcing MD before VDE evolves and prevent severe plasma vertical instabilities with large halo currents in the plasma surrounding conductive structures;
- act against the severe generation of runaway electrons.

It is assumed that this system will cause disruptions with time duration of the CQ of 50-150 ms which corresponds to the time duration of a MD I event.

In the load combination of concatenated events the worst, but still conceivable, time evolution of the loads shall be taken into account. In many cases even if events are concatenated, maximum loads cannot physically occur at the same time. In each of these cases the proper scaling of the maximum loads has to be considered in the load combination. Examples are:

- plasma transient event (26-500 ms time scale) triggering a magnet fast discharge of any type (several seconds time scale);

- plasma transient events triggering VV ICE (pressure and temperature increases in the VV due to VV ICE have time scale of hours);
- VV ICE triggering plasma transients

For what concerns the concatenation of plasma transient events triggering magnet fast discharge, in addition to the fact that the loads associated to each single event are not concomitant, these load combinations are generally enveloped by the combination of event sequences where the magnet fast discharge transients trigger the plasma transient events. Some of these combinations are herein listed. Other concatenations of plasma transient events with magnets fast discharge events will be considered for the magnet design.

For the combination of seismic events with machine operation loads it is taken into account that the plants has a seismic detection system that stops operation as ground motions due to incoming seismic event is detected.

The seismic events shall be considered occurring when the machine is in plasma operation status or in another possible status (e.g. baking) if this represents a worst condition.

In the cases of seismic events combined with other accident conditions (e.g. Cr ICEs) the loads are conservatively considered concomitant in time to account for seismic aftershock (a second seismic shock that follows a previous seismic event responsible of the accident condition).

When loads are considered concomitant, unless otherwise specified, the maximum values of the responses are combined algebraically. This is a conservative assumption considering the dynamic nature of certain specific loads (examples: EM loads due to plasma transient and seismic loads). A different combination method needs to be justified.

It is here assumed that:

- it is ‘Probable’:
  - ⇨ for an SL-1 seismic event to trigger a MD I;
  - ⇨ for an SL-1 seismic event to trigger a MFD I or a MFD II;
  - ⇨ for any magnet fast current discharge (MFD I or MFD II) to trigger a MD I;
  - ⇨ for any in-vessel ICE to trigger a MD I;
  - ⇨ for a VV ICE II or III to trigger MD II;
  - ⇨ for a VV ICE III or IV to trigger a MD III;
  - ⇨ for a VV LOVA III to cause a MD III;
  - ⇨ For a SMHV to cause Cr ICE III or Helium Leak in Gallery;
  - ⇨ for a SL-2 to cause a loss of Off-site power (LOOP);
  - ⇨ for a SL-2 to cause a failure in power supply (internal AC or DC);
  - ⇨ for a SL-2 to cause Cr ICE III, or Helium Leak in Gallery, or Internal Fire;
  - ⇨ for any Cr ICE or Cr LOVA to trigger a MFD I or II;
  - ⇨ for a MD II or a VDE II to cause a VV ICE II
  - ⇨ for a MD III or a VDE III to cause a VV ICE II or III;
  - ⇨ for a MD IV or a VDE IV to cause a VV ICE III or IV;
  - ⇨ for a VDE III to trigger a MFD I.

- It is 'Conceivable':
  - ⇨ for an SL-1 seismic event to trigger a MD II or III or VDE II;
  - ⇨ for any magnet fast current discharge (MFD I or MFD II) to trigger a MD II;
  - ⇨ for any magnet fast current discharge (MFD I or MFD II) to cause a VDE II (It is assumed conceivable and not probable as the DMS is acting to prevent VDEs);
  - ⇨ for a MFD II to cause a Cr LOVA III;
  - ⇨ for a VDE II to cause a VV ICE-III;
  - ⇨ for a MD II to cause a VV ICE-III;
  - ⇨ for a MD III or VDE III to cause a VV ICE-IV;
  - ⇨ for a MD III to trigger a MFD I;
  - ⇨ for VV ICE II to trigger a MD III (combination in category III);
  - ⇨ for a SL-1 to trigger a MD II and MFD II;
  - ⇨ for a SL-1 to trigger a VDE II and MFD II;
  - ⇨ for a SMHV to trigger an internal fire.

The low probability of a VV ICE to cause a VDE brings this concatenation of events beyond design basis.

The low probability of a VV ICE III and VV ICE IV to cause a MD IV brings these concatenations of events beyond design basis.

The low probability of a VV LOVA III to cause a VDE brings this concatenation of events beyond design basis.

The low probability of a VV LOVA III to cause a MD IV brings this concatenation of events beyond design basis.

Table 5-1: Load Combinations and Their Categories

Pressure	Seismic	Plasma	Magnet	Others CatI (1)	Others CatII (1)	Others CatIII (1)	Others CatIV (1)	Cat	# of events (2)
		MD I		P				I	2600 (3)
			MFD I	P				I	500 (3) (4)
		MD I	**MFD I**	P				I	500 (3) (4)
		MD II		P	P			II	400 (3)
		VDE II		P	P			II	300 (3)
			MFD II	P	P			II	50 (3)
		MD I	**MFD II**	P	P			II	50 (4)
		MD II	**MFD I**	P	P			II	50 (3)
		VDE II	**MFD I**	P	P			II	50 (3)
VV ICE II		**MD II**		P	P			II	15 (3)
VV ICE II		**VDE II**		P	P			II	15 (3)
VV ICE II				P	P			II	15 (3)
VV ICE II		MD I		P	P			II	15 (3)
VV ICE II		MD II		P	P			II	15 (3)
Cr ICE II				P	P			II	15 (3)
Cr ICE II			MFD I or II	P	P			II	15 (3)
	SL-1			P	P			II	1 (5)
	SL-1	MD I		P	P			II	1 (5)
	SL-1		MFD I or II	P	P			II	1 (5)
	SL-1	MD I	MFD I or II	P	P			II	1 (5)

VV ICEIII		**MD II**		P	P	P		III	-
VV ICEIII		**VDE II**		P	P	P		III	-
		MD III		P	P	P		III	-
		VDE III		P	P	P		III	-
		VDE III	MFD I	P	P	P		III	-
VV ICE II or III		**VDE III**		P	P	P		III	-
VV ICE II or III		**MD III**		P	P	P		III	-
		MD II	**MFD II**	P	P	P		III	-
		VDE II	**MFD II**	P	P	P		III	-
Cr LOVA III			**MFD II**	P	P	P		III	-
VV ICE III				P	P	P		III	-
VV ICE II		MD III		P	P	P		III	-
VV ICE III		MD I		P	P	P		III	-
VV ICE III		MD II		P	P	P		III	-
VV ICE III		MD III		P	P	P		III	-
Cr ICE III				P	P	P		III	-
Cr ICE III			MFD I or II	P	P	P		III	-
Cr LOVA III				P	P	P		III	-
Cr LOVA III			MFD I or II	P	P	P		III	-
VV LOVA III				P	P	P		III	-
VV LOVA III		MD III		P	P	P		III	-
VV LOCA III				P	P	P		III	-
	SL-1	MD II		P	P	P		III	-
	SL-1	VDE II		P	P	P		III	-
	SL-1	MD II	MFD-II	P	P	P		III	-
	SL-1	VDE II	MFD-II	P	P	P		III	-
	SMHV			P	P	P		III	-
Cr ICE III	**SMHV**			P	P	P		III	-
Cr ICE III	**SMHV**		MFD I or II	P	P	P		III	-
He in Gallery	**SMHV**			P	P	P		III	-
LOCA GalleryIII				P	P	P		III	-
LOCA_PC III				P	P	P		III	-
LOCA_NB III				P	P	P		III	-
Helium leak in galleries				P	P	P		III	-
IVC LOFA III				P	P	P		III	-
		VDE IV		P	P	P	P	IV	-
		MD IV		P	P	P	P	IV	-
VV ICE III or IV		**VDE IV**		P	P	P	P	IV	-
VV ICE III or IV		**MD IV**		P	P	P	P	IV	-
VV ICE IV		**MD III**		P	P	P	P	IV	--
VV ICE IV		**VDE III**		P	P	P	P	IV	--
VV ICE IV				P	P	P	P	IV	-
VV ICE IV		MD I		P	P	P	P	IV	-
VV ICE IV		MD II		P	P	P	P	IV	-
VV ICE IV		MD III		P	P	P	P	IV	-
		MD III	MFD I	P	P	P	P	IV	
Cr ICE IV				P	P	P	P	IV	-
Cr ICE IV			MFD I or II	P	P	P	P	IV	-
Int. fire	**SMHV**			P	P	P	P	IV	-

	SL-1	MD III	P	P	P	P	IV	-
Cr ICE III	**SL-2**		P	P	P	P	IV	-
He in Gallery	**SL-2**		P	P	P	P	IV	-
Int. fire	**SL-2**		P	P	P	P	IV	-
LOOP	**SL-2**		P	P	P	P	IV	-
Int. fire			P	P	P	P	IV	-
LOCA in Vault			P	P	P	P	IV	-
LOCA PC III + VV ICE II			P	P	P	P	IV	-

(1) Other load conditions, which are peculiar to single components and are defined in the specific SRD[1] or DDD[2] documents.

(2) Unless a detail dynamic analysis is performed and the number of cycles per event is directly calculated, it is recommended to assume for each seismic event 10 equivalent maximum stress cycles whenever a fatigue or a cyclic load analysis is required. For disruptions and VDEs the number of equivalent cycles per event has to be determined based on the dynamic response of each single component. Category III events and combinations shall be assumed to occur once in the machine life unless otherwise specified.

(3) This number is reduced if this event is combined with other events (examples MD + MFD, MD + ICE, etc.). The reduction corresponds to the number of events assumed in the additional combinations.

(4) This number include also events in which MFDs are triggered by MDs or VDEs

(5) As this event has a return period of more than 100 years it is expected to occur only once in the machine life. If required by investment protections it shall be assumed to occur a maximum number of 5 times.

Conditions in bold characters are the initiating conditions. The *'P'* character stands for *'Probable'* for what regards the correlation between the initiating event and the consequently combined other events.

The above table is referenced and applied within the different components design assessments (SR or DDD's). General conditions are specified further ahead in this chapter while most loading conditions, typically affecting only a single component, are addressed in the specific DDD or in the specific System Load Specification Documents.

The following additional accidental events combinations need to be considered. They affect mainly the design of the building. They do not need to be combined with electromagnetic transient and seismic events. In bold the initiating event is indicated.

[1] System Requirement Document

[2] Design Description Document

Table 5-2: Additional fault conditions (*)

Event	Category
LOCA Vault IV	IV
Internal fire + **Internal explosion**	IV
Internal fire + internal Flooding	IV
LOCA + Internal Flooding	IV
Air crash + external fire	IV
Water table + external flooding	IV
External fire + **external explosion**	IV
Accidental temperature + external fire	IV
Internal explosion + load drop	IV
External Fire + External Explosion	IV
Internal Explosion + Internal flooding	IV
Internal Fire + Internal Explosion	IV
Damaged equipment + Internal flooding	IV

(*) items in bold represent the initiating event

The following additional load case combinations are classified in category V and need to be considered for the design and verification of the second safety confinement barrier. The service level (allowable and limit load values) are defined following safety requirements.

Table 5-3: Load combinations in category V to be considered for the design and verification of the second safety confinement barrier. (*)

Event combination	Category
MFD II + VDE IV	V
Cryostat air ingress + MFD II + VDE II	V
VDE IV + VV ICE IV	V
Cr ICE IV + MFD II + VDE II	V
VDE IV + MFD I	V
SL-2 + Cr ICE IV (from Magnets and Thermal Shield) + ICE III in gallery + MFD II + VDE II	V
Cr ICE V (water leak inside the cryostat)	V

(*) items in bold represent the initiating event

6 General loads description

Part of the technical difficulties associated with the design of the ITER tokamak is due to the substantial mechanical loads which can develop in multiple components. This subsection will briefly describe the main static and transient loading conditions which concern the ITER design.

The loads acting on ITER can be divided into five different types:

1. *Inertial loads*: these are due to accelerations due to gravity and seismic events.
2. *Pressure loads*: significant on the ITER vessels, include fluid pressure (e.g., Vacuum Vessel cooling water), and externally applied atmospheric pressure to vacuum (e.g., Cryostat Vessel).

3. *Electromagnetic loads*: these are normally a strong design driver and not only affect, in their static form, the magnet system (e.g., TF magnet) but also act upon nearly all conductive structures during fast transients (e.g., plasma disruptions and resulting induced currents on the in-vessel components).
4. *Thermal loads*: these often induce stresses (e.g. those caused by constrained thermal expansion), typically circumscribed within a single component and thus not giving rise to significant global effects (ITER components supports are generally designed to allow free thermal expansion).
5. *Assembly loads*: loads applied to components during the assembly phase (e.g. preload on magnets)

In order to better describe the mechanical loads from a system point of view it is worth briefly describing the general layout of the main component supports.

The general arrangement of supports of the tokamak components has been developed to allow thermal expansion in order to minimise thermal stresses.

- The TFC supports consist of flexible plates resting on a ring (the pedestal ring). The flexibility of the plates allows free radial expansion, but reacts against toroidal forces.
- The Vacuum Vessel is vertically and toroidally supported at the lower ports. These supports are attached to the pedestal ring and allow free thermal expansion by the presence of a double hinges system. The supports are inclined against the vertical direction by a small angle which causes a small vertical VV movement associated to temperature changes. Sideways net loads on the VV are transferred to the pedestal ring through toroidal reaction forces. In addition to this mechanical support system, the VV is magnetically coupled to the TF coils. When the TF coils are energised, the VV is fully immersed in the toroidal magnetic field. As a consequence, any horizontal relative movement of the VV with respect to this magnetic field (and therefore to the TF coils) is reacted by an opposing force. This effect is mechanically equivalent to a horizontal stiffness in series with a damper that in this document are called magnetic VV/TFC stiffness and damping.
- CS, PF, and CC coils are supported through the TF gravity support system.
- The in-vessel systems (blanket modules, divertor) are directly supported by the Vacuum Vessel.
- Magnets and VV supports are resting on the pedestal ring that is part of the cryostat

The pedestal ring is supported vertically by the basemat. Horizontal forces on the tokamak main components are transferred from the pedestal ring, the cryostat horizontal plate, the cryostat skirt, and the horizontal lugs to the bioshield. The horizontal lugs are designed to transfer 100% of the horizontal loads from the tokamak to the building.

The support hierarchy can therefore be schematically drawn as follows:

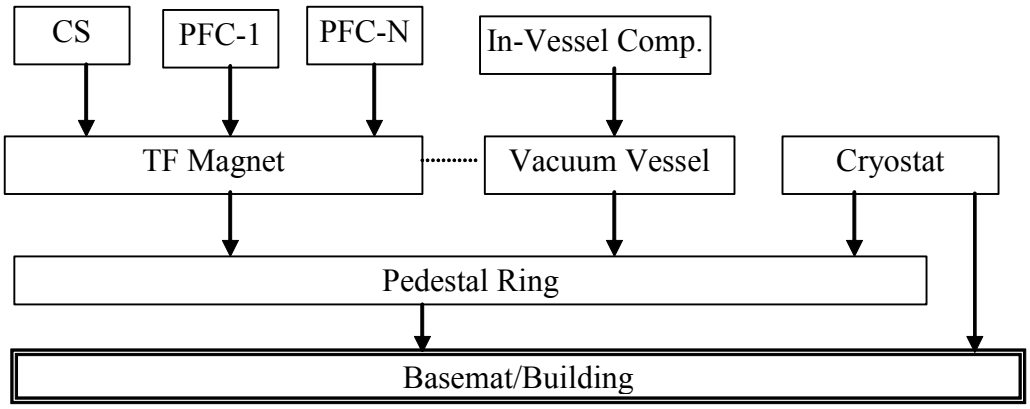

Figure 6-1 Schematic of Supports Hierarchy

Only two PF coils are schematically shown in order to simplify the diagram which will be here used to show the mechanical load paths.

6.1 Seismic loads

An earthquake consists of an oscillatory movement of the earth's surface. The ground acceleration can be both in the horizontal and in the vertical direction and typically has a spectral content which leads to some level of support reaction load amplification.

A seismic event is, in many cases, the most demanding loading condition, in particular for the supports and interface structures which must be sized for high strength, and often also for high stiffness.

The load path during a seismic event can be visualized as shown in Figure 6-2 (in the picture the basemat is isolated from the ground by the seismic isolators).

In that picture the magnetic VV/TF Magnet coupling is shown. This coupling stiffness is considered only when the magnets are energised that means only in the load case combination of seismic loads with other operational loads.

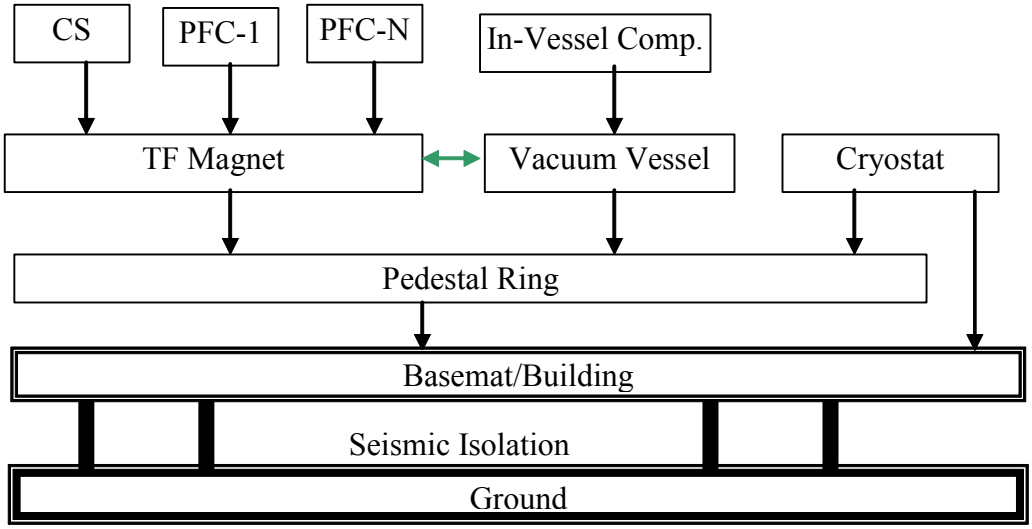

Figure 6-2: Load Paths during a Seismic Event

6.2 Electromagnetic loads, slow transients

Energies in excess of 40 GJ are normally stored in the ITER superconducting magnet system in the electromagnetic fields that provide plasma stability, plasma equilibrium, and drive current in the plasma. Associated with the provision of such strong fields, considerable magnetic loads have to be reacted by the magnet assembly.

6.2.1 TF magnet loads

During normal operating conditions, the TF magnet system has to withstand the EM loads arising from the interaction of its conductor current with both the Toroidal and Poloidal fields.

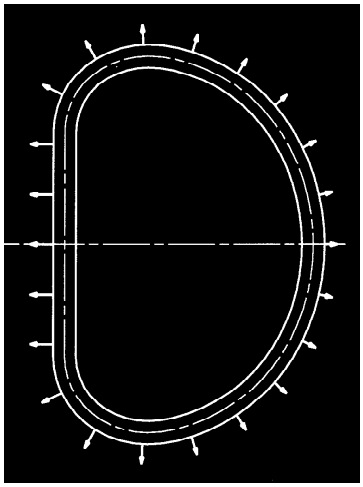

Figure 6-3: In-Plane Loads on a TF Coil

The interaction with the toroidal field gives rise to a force (see Figure 6-3) acting in the plane of the each coil, and which can be pictured as a pressure acting from the Vacuum Vessel side outward with an intensity which reduces as the radial position increases.

As a consequence of this load distribution, each coil experiences a strong internal tension as well as a radially directed inward force which is reacted in hoop compression by the TF magnet itself as it behaves as a vault in its inboard region.

This load is basically internal to the TF magnet assembly in that no *net* loads are transmitted onto other components.

The interaction of the TF magnet current with the poloidal field, present only during plasma operation, gives rise to a load which is normal to the plane of each coil. This load does not produce a net moment around the vertical axis of the machine but tries to twist the whole TF magnet with opposing sign toroidally directed forces. While being a load of somewhat smaller intensity, when compared with the in-plane load, is of a pulsed nature.

The reaction of this load is accomplished by the TF coil cases, their different intercoil structures, which increase both stiffness and strength of the magnet assembly.

6.2.2 CS and PF magnets loads

The CS and PF magnet systems produce the poloidal magnetic field necessary for plasma equilibrium and shaping, as well as the toroidal electric field needed to build and sustain the plasma current. The forces acting on the CS and PF coils are radially and vertically directed and are essentially axisymmetric (expect for the small ripple effect of the discrete TF coils).

The load on CS and on each PF coil greatly varies as a function of other coil currents, plasma current, plasma profiles, etc. Therefore, in order to size its supporting structures, the envelope of all conditions must be considered.

During slow transients (e.g., plasma initiation, shutdown, etc.), the *net* force on the whole PF magnet system is nearly zero due to the substantial absence of induced currents in the passive structures (VV, Blanket, etc.).

Net vertical loads are exchanged between different PF coils through the TF magnet structure but without affecting its supports to ground or to the Vacuum Vessel.

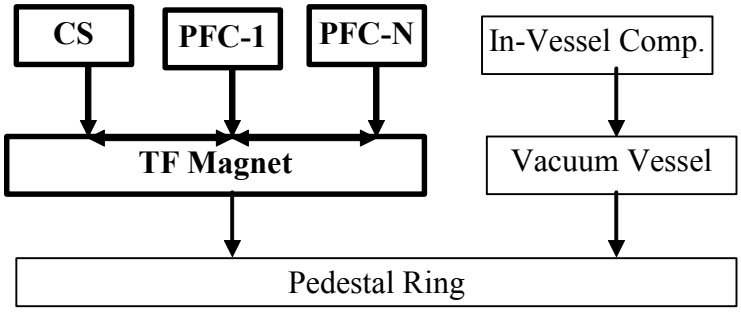

Figure 6-4 Load Paths between PF Coils

6.3 Electromagnetic loads, fast transients

Electromagnetic fast transients will occur, in ITER, and the consequent loads must be considered for the design of the ITER components.

The main consequence of these transients is the induction of currents in the conducting structures which, in turn, give rise to significant internal and mutual loads.

6.3.1 Disruptions

In a plasma disruption the plasma thermal energy and current are rapidly reduced to zero as a consequence of loss of confinement and impurity influx.

If such a plasma current quench (CQ) takes place in a time short (e.g., < 100 ms) compared with the vertical resistive plasma motion (200-300 ms) it would be expected that significant total net vertical forces are not generated (compared to the case of a full blown VDE) in the whole of the passive structure. However, as induced eddy currents in the upper and lower parts of the plasma surrounding structures are different due to the up/down asymmetry, the plasma may move either upward or downward inducing halo currents and vertical forces. The magnitudes of these forces are, anyway significantly smaller compared to the full blown VDEs.

A significant poloidal current may also flow in the passive structure as a consequence of the occurring variation of toroidal flux (during thermal (TQ) and current quench) as well as poloidal flux during current quench. This current leads to loads internal to the vessel and the conducting structures around the plasma without significant force exchange with the magnet. Nonetheless, given the up-down asymmetric coupling of the ITER plasma with the passive conducting structure, significant plasma fast vertical displacements may take place. The direction of plasma movement after the TQ strongly depends on the initial equilibrium vertical position of the plasma current centre,Z_{cur} . Since the impact of vertical displacement on the machine due to eddy and halo currents is much more severe for a downward displacement (toward the X point) than upward, the initial equilibrium vertical position Z_{cur} is specified somewhat above the global tokamak zero vertical position to ensure that, for many of the disruptions, the plasma movement is in the upward direction. However, the direction also depends on the change of the internal inductance (ℓ_i) at the TQ as well as the current quench rate during the current quench phase. Therefore, both upward and downward movement must be considered for the EM load analysis.

This type of events has been named at the beginning of the ITER design phase Central Disruption (CD) to indicate that the plasma thermal quench starts with the plasma close to the central equilibrium position. Subsequently the name has been changed to Major Disruptions (MD), because simulations indicated that vertical displacements of the plasma can occur during the plasma current quench. These names can be found in the ITER documentations to identify the same phenomenology.

The main structural consequence of the plasma disruption is the induction of local loads on the blanket modules, vacuum vessel, and plasma facing components.

The severity of this event strongly depends on the assumption on the total current quench duration.

The disruption can be considered to be divided into two classes with different EM load consequences depending on the characteristics of current quench:

- the first is a disruption with a TQ followed by a fast current quench time;
- the second is a disruption with a TQ followed by a current decay that is considered slow at the beginning and turn to be fast at the end (MD slow_fast = MD SF).

In the first case only small plasma current remains when plasma moves upwards or downwards significantly and only small halo current is exchanged between plasma and surrounding structures.

In the second case the plasma, after the TQ, becomes vertically unstable and drift vertically [40]. The evolution of halo current and forces exerted on surrounding structures is comparable to a VDE case.

Plasma disruptions with slow plasma current quench decays generate loads that are smaller with respect to those generated by fast plasma current decay or VDEs. For this reason the loads that they generate are considered enveloped by the mentioned events and are not required to be considered for the design of ITER components.

6.3.2 VDEs

In a Vertical Displacement Event (VDE) the vertical position control of the plasma is lost as a consequence of a failure of the feedback control system. The plasma motion, in this case, may take place without initial significant plasma current reductions (current quench) and would progress relatively slowly (in the time scale of the vertical resistive mode of the passive structure).

The VDE is composed of an initial slow vertical drift phase and onset of plasma-wall contact followed by the onset of a disruption and/or rapid loss of remaining plasma thermal energy. The halo current and thermal quench may start as soon as the plasma comes in contact with the first wall. As plasma moves further after contacting the wall, edge safety factor q_{edge} continues to decrease. However, even if TQ did not occur during this movement, TQ will inevitably occur before and when q_{edge} reaches the critical value of 1.5 below which plasma MHD stability is assumed absolutely violated. EM loads will be largest when TQ occurs at q_{edge} = 1.5, which can be categorized as the most severe case.

Since VDEs terminate with a plasma current quench, their severity is rather dependent on the delay between the onset of the VDE and the onset of the current quench as well as the duration of the latter. As the onset of the current quench is delayed, the plasma moves further into the destabilizing quadrupolar field and finds his equilibrium by interacting with the surrounding conductive structures.

The plasma vertical instability causes a plasma vertical movement which is slowed down by a transfer of current from the plasma to the passive structure. This passive stabilizing effect is due to both the induced currents and the halo current which is a direct exchange of current from the plasma to the interacted structures.

As the plasma has a negligible mass, it must be in equilibrium during the full transient event, but the VDE typically gives rise to significant net forces between the CS and PF magnets and the passive structure.

The vertical force balance during VDE events can be explained somewhat in more detail as follows. When the plasma suffers any vertical displacement from the equilibrium position for any reason (assumed downwards for the purposes of this discussion) the plasma receives a downward force ($F_{p,c}$ in Fig. 6-5) from the radial component of magnetic field necessary for the plasma elongation, which further accelerates the downward motion (vertical displacement event; VDE). At the same time, a poloidal halo current flows outside of the last closed flux surface (halo region), generated by the compression of the toroidal flux within the plasma as it moves towards the vessel. This poloidal halo current generates the upward force (F_h in Fig. 6-5) on the plasma and decelerates the downward plasma movement. The halo region intercepts the vessel and thus the halo current flows into the vessel, which generates the downward vertical force ($F_{v,h}$ =-F_h in Fig. 6-5). The vertical force on the plasma and the vessel due to the halo current is generated by the coupling between the toroidal magnetic field and they are of exactly same magnitude but opposite direction. Thus the reaction force on the toroidal coil exactly cancels out and no net force acts on the TF coil during VDEs.

In addition to the halo current force, eddy currents are induced on the vacuum vessel due to the plasma movement and plasma current decay. An additional vertical force is generated due to

the coupling of this induced eddy current with the poloidal field from PF coils ($F_{v,c}$ in Fig. 6-5) and the plasma ($F_{v,p}$ in Fig. 6-5). Thus, the force on the vessel due to the induced eddy current, F_{eddy}, is the sum of these two forces; $F_{eddy} = F_{v,c} + F_{v,p}$. The direction of this force depends on the speed of movement and current decay, and generally changes its sign in time.

Total force on the vessel is therefore the sum of the forces due to the halo current and the eddy currents. Since the total force acting on the plasma is always 0 (quasi-equilibrium since disruption time scale is much longer than poloidal Alfvén time scale), the following force balance holds:

$$F_h + F_{p,v} + F_{p,c} = 0 \quad [1]$$

Therefore, the total force on the vessel is expressed as

$$F_v{}^{total} = F_{eddy} + F_{v,h} = F_{p,c} + F_{v,c} \quad [2]$$

Thus, the reaction force acts only on the PF coils.

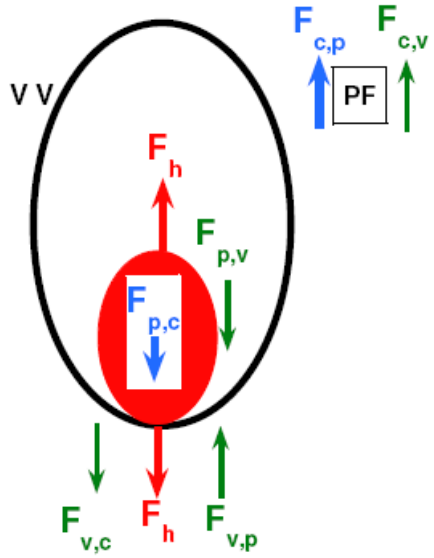

Figure 6-5 Schematics of vertical force balance during VDEs

The VDE can be considered to be divided into three classes with different EM load consequences depending on the characteristics of current quench:

- the first is a VDE followed by a fast current quench time that results in the higher eddy currents on in-vessel components and vacuum vessel;
- the second is a VDE followed by a slow current quench time that results in the higher halo currents and vertical loads on the structure;
- the third is initially slow and later fast (slow_fast), which results in significantly large loads due to both halo and eddy currents.

The current quench time depends mainly on the core and halo temperature. A lower core/halo temperature leads to higher resistance in the plasma region and results in the fast VDE and lower halo current, and the higher one results in the slow VDE and higher halo current.

For the modelling of fast, slow and slow_fast current quench types of VDEs the initial scenario is the same. The vertical control system is deactivated and the plasma is given, from its initial unstable equilibrium point, a small initial upward or downward kick. The plasma then drifts in the direction of the displacement and rapidly becomes limited by the first wall. The plasma remains limited and shrinks in cross-section while maintaining its current as it continues to drift. During the drift phase, which typically lasts ~0.5 s, no power is supplied to the plasma

and the plasma energy slowly decays at a rate determined by the thermal transport in the equilibrium state.

It has also been observed, in present experiments, that in many cases during current quench, induced poloidal halo current is not toroidally uniform. This is expressed by the toroidal peaking factor (TPF). This toroidal asymmetry is considered to be generated by the plasma kink instability.

Large toroidal asymmetry of the toroidal plasma current has also been observed, especially in JET, which indicates that asymmetric toroidal current flows in the vacuum vessel. Associated with this asymmetric toroidal current, large horizontal load has also been observed. This asymmetry toroidal current has a clear correlation (90° phase shift) with the asymmetry poloidal halo current, and thus, it is considered they are generated by the same origin, which suggests that both asymmetries of poloidal halo and toroidal currents should occur always for the EM load analysis. This is taken into account by defining the maximum horizontal forces on VV and magnets and toroidal peaking factor for the poloidal halo current distribution. The asymmetry halo and plasma currents can rotate in toroidal direction and can trigger repetitive cyclic loads, which can lead to large dynamic amplification factors.

The understanding of these phenomena is not fully clear and their modelling is still somewhat primitive. Nevertheless the design guidelines have been established for ITER (discussed ahead in Appendix I and section 7.3.3.2) based on phenomenological observations and statistic database.

6.3.3 Magnet system discharges

A magnet fast discharge (MFD) is an event where the current flowing in the magnet (TF, PF, CS, CC or all) is rapidly brought to zero by means of discharge resistors which dissipate the large stored magnetic energy. Such an event is usually triggered by the magnet quench detection systems which intentionally do so to protect the conductor from overheating.

Two different type of MFD are defined:

a) MFD I which corresponds to a fast discharge of the CS and PF coils only,
b) MFD-II which correspond to an event in which all the superconducting coil systems are discharged.

As a consequence of the decay of the poloidal field in a MFD I, as the CS and PF coils are discharged, a toroidal electric field is generated and eddy currents are induced in the passive structures. These are similar to those generated during plasma initiation. During the transient some net loads have to be reacted between the passive structures and the CS and PF magnets. The superconducting coil decay time function in the MFD I event are defined in DDD 11-3.

When the toroidal field is discharged in MFD II, much larger loads occur in the Vacuum Vessel and in-vessel components as a consequence of the changing toroidal field which generates a substantial poloidal electric field. Due to toroidal symmetry of the magnetic field variation during the transient (all TF coils are connected in series and current values and derivatives are the same in each coil), the majority of loads are reacted within the passive structures or the coils and no significant net loads (on TFC and VV supports) have to be reacted.

6.4 Heat Loads

Unconfined plasma energy during normal operation and plasma disruptions is discharged on the surrounding mechanical structures.

The main energy transfer mechanisms are nuclear radiation, thermal radiation, and physical impact of particles (conduction and convection).

Large thermal energy is transferred from the plasma to the surrounding structures in case of plasma thermal quench, plasma current quench, plasma drift to first wall, and runaway electrons. Detailed specifications for the heat and nuclear loads are provided in [2].

6.5 Vacuum Vessel ICE

The VV Ingress of Coolant Events (ICEs) includes:

- pipe breaks and leakages from the blanket, divertor or other in-vessel components;
- ingress of cryogenic coolant inside the VV.

The description and analysis of the scenarios is reported in AAR Volume I and II [23 and 24].

Following the ITER classification strategy of events, VV ICEs are classified in three distinctive categories (II, III, and IV). The full list of postulated events and their category is defined in table 6.1-1 of [23]. Major assumptions for these events are as follows:

6.5.1 VV ICE-II

For this type of event the worst conditions correspond to a discharge from 1-10 coolant channels (e.g. caused by plasma induced damage or a crack in the pipe from a flaw, from thermal and mechanical overstress, or from erosion-induced wall thinning) of First Wall. In this event, coolant is discharged at a relatively low flow rate directly into the vacuum vessel (VV), causing the plasma to disrupt very quickly.

This event envelopes all types of small anticipated in-vessel loss-of-coolant leaks that may threaten the VV confinement boundary.

6.5.2 VV ICE-III

For this type of event the worst conditions correspond to a discharge from multiple coolant channels affecting 1 PHTS loop of the First Wall (e.g. caused by runaway electron initiated damage) or few coolant channels of divertor or other in-vessel components.

6.5.3 VV ICE-IV

For this type of event the worst condition corresponds to a discharge from multiple PHTS loops (e.g. caused by severe runaway electron).

6.6 Cryostat ICE

Pressurization of the cryostat can occur if cryogenic helium or water is expelled into the cryostat.

Various sized helium leaks are assumed and they are classified in category II, III and IV. A water ingress event inside the cryostat is considered beyond design basis (load category V) as all water pipes inside the cryostat have guard pipes.

The description and analysis of the scenarios is reported in AAR Volume II [24] sections 3.7.2 and 3.7.3.

6.7 Loss of vacuum inside the VV (VV LOVA)

The large number of penetrations inside the VV has motivated the investigation of a loss of vacuum with air ingress through a confinement bypass as one of the Accidents. The generic

bypass assumes an opening of 0.02 m^2, representative of the sizes of ICRF, ECRF, fuelling lines, in vessel viewer, and some diagnostics.

The description and analysis of the scenarios is reported in AAR Volume II [24] section 3.2.2.

6.8 Loss of vacuum inside the Cryostat (Cr LOVA)

Cryostat leaks are investigated as accidents. A maximum leakage is postulated to be 0.2 m^2 that is estimated on the basis of a bellow failure. This event is classified in category III.

The description and analysis of the scenarios is reported in AAR Volume II [24] section 3.7.1.

6.9 Loss of Coolant Accident (LOCA) outside the cryostat

Four different types of LOCA outside the cryostat are considered depending on the location of leak:

- Ex-vessel LOCA in galleries (VV coolant) – reference event X4, according to [24] - section 3.3.3.
- Ex-vessel LOCA in port cell (blanket coolant) – reference event X8, according to [24] - section 3.3.5.
- Ex-vessel LOCA in NB cell.
- Ex-vessel LOCA in vault (divertor coolant) – reference event X5, according to [24] - section 3.3.4.

These events can occur either during plasma operation or during baking.

If the event occurs under plasma operation conditions a major disruption may be triggered (either by the Fusion Power Termination System or due to the ingress of gas into the VV chamber). It is assumed that the break is coincided with loss of off-site-power for 32 hours, hence active cooling of the in-vessel components is lost.

6.10 Loss of forced flow accidents (LOFA) in VV and in-vessel components

For the VV, the following Loss Of (Forced) Flow Accidents (LOFA) has been considered:

- Loss of forced flow in the VV cooling loop and additional failure of the low-flow pump powered by emergency diesel generators. This event is classified beyond design basis (category V).

For the in-vessel components (blanket and divertor) the postulated accident corresponds to the loss of forced flow in one loop of first wall/blanket/ divertor due to loss of site power or pump failure.

6.11 Helium Ingress in Galleries

This event is described in [39]. It concerns a spillage of cryogenic coolant from the magnet cryogenic cooling loop inside the cryostat space room, which is assumed connected to the gallery. This event may occur during plasma operation, between pulses or during a shut-down period with vacuum in the cryostat being maintained.

6.12 Loss of power

The assumed maximum duration of a Loss Of Off-site electrical Power (LOOP) is 32 hours.

A more frequent (incident) short duration (1-hr) LOOP and a 1-hr power station blackout (accident) with simultaneous loss of diesel motor generator (voltage class III) and loss of off-site power (voltage class IV) are also to be analysed.

In case of Loss Of Off-site Power (LOOP) for 32 hours the pumps of the primary coolant loops and in the heat rejection system loops for the first wall/blanket and divertor are tripped and coast down. The plasma terminates within a few seconds either from active plasma termination due to low flow signals in the primary cooling loops or from interruption of fuelling. The water coolant will be slowly heated due to decay heat inside the structures. Pressure relief valve in the Primary Heat Transport System (PHTS) opens to expel the coolant after a few minutes. This coolant will be safely captured in drain tanks.

6.13 Internal Fire

The severity of the event of an internal fire will be specified individually for each room following an adequate assessment of the materials present in each room. The severity of a fire event is defined by the expected maximum temperature and the duration of the event. Simultaneous fire in more than one room does not need to be considered. Since it is specified that no fire event will occur inside the bioshield only the following first confinement barrier systems are affected:

- VVPSS tank, relief line, oblong pipe, rupture discs and safety valves on “bleed bypass lines”
- NB injector and bellows to VV duct
- TCWS pipes
- Regeneration / roughing lines
- Pellet injector
- EC launcher - equatorial / upper port plug

6.14 Internal Flooding

Internal flooding does not affect the design of the components inside the tokamak complex. The possible spillage of water due to:

- Cooling loops
- Fire suppression system

will be collected by an adequate tank or by the rooms themselves for which a liquid leak tightness is required.

6.15 Internal Explosion

An internal explosion [24] affecting tokamak and first confinement barrier components is defined as *beyond design*.

In case of air ingress inside the VV, deflagration or detonation of the hydrogen/air mixture is not studied, as it is proposed that the ITER design will contain provision for prevention of such an explosion, for example by injection of an inert gas into the vessel (ref [24] par. 3.3.5).

6.16 Load Drop

Appropriate measures will be taken in the design of the components in the tokamak building, the assembly and remote handling tools to ensure that components will be protected from load drop.

6.17 (Damaged) Equipment

Appropriate measures will be taken in the design of the components in the tokamak building to ensure that a failure of a component, e.g. break of pipe, will not trigger failure to surrounding components, especially those that are SIC classified.

6.18 System fault conditions

In previous chapters several fault conditions have been described. These are fault conditions that have been considered in the ITER Rapport Préliminaire de Sûreté (RPrS) [22] and in the AAR [23, 24, 25]. These events have an impact on the overall plant or to several SSC (System, Structure, and Component). It has to be considered that each SSC might have other specific fault conditions that do not affect the overall plant, but will have local effects that need to be considered. Examples of these specific faults are:

- Failure of one or more supports
- Leaks or pipe breaks internal to specific systems
- Electrical shorts
- Degradation of functions (electrical insulation, loss of preloads, degradation of frictions or sliding, etc.).

These specific faults shall be identified by performing a hazard or risk analysis of each specific system.

These load conditions and the concatenation with other events shall be described in the system documents (SRDs, System Load specification, etc.).

6.19 External Loads Acting on the Nuclear Buildings

All load events listed in the table below are reacted by the building in such a way that no loads are seen in these events by the internal components:

Table 6-1: List of exceptional events to be considered in the building design

Load Event	Description
External fire	The external building walls are designed to withstand the specified external fire event.
External flooding Water table	The foundation of the tokamak building is designed to withstand the specified water table and the specified type of external flooding.
External explosion	The external building walls are designed to withstand an overpressure of 50 mbar.
Airplane crash	The external building walls are designed to withstand the general aviation. Although an airplane crash event can cause an internal fire event, any propagation of fire is avoided through the collection of the fuel.
Accidental temperature	The tokamak building is designed for external temperatures in the range [-15°C; 40°C]. In case external temperature occur outside this range within the specified limits, only the building external walls will be affected, the building interior will remain temperature controlled, hence no excessive thermal expansion occurs at internal walls.

7 Loading conditions specification

In the following paragraphs particular conditions, which involve multiple systems, are specified and classified. A more detailed discussion of the loading of individual systems under these conditions is included in the SRD or DDD or technical specification documents of the relevant component or system.

7.1 Seismic events

Seismic events shall be considered to occur during plasma operation assuming the machine in the worst foreseeable conditions. For each system and component the worst foreseeable condition has to be identified. It has to be considered that for different systems or parts of a system the worst condition can be represented by different conditions or machine status.

Seismic events SL-2 and SMHV (see 7.1.1) do not need to be considered during initial machine assembly or during first installation for the following reasons:

- there is no handling of nuclear components or activated product;
- the assembly status is continuously evolving and lasting relatively short time;
- no regulation in France is requesting seismic verification during assembly.

During assembly the structure and assembly tools have to be secured for possible horizontal actions.

It has to be noted that for investment protection the design and verification of structures and assembly tools for SL-1 (or other seismic level) event may be required for assembly phase based on IO decision. This requirement will be specified in the SRD or in the System Load Specification Document.

7.1.1 Ground accelerations

Seismic load excitation corresponds to the specific selected site for the ITER construction (Cadarache) [7]. For buildings and equipment that are classified in seismic class 1 and 2 (SC1 and SC2) [3] three levels (SL-2, SMHV and SL-1) of ground motion are considered.

SL-2 corresponds to the seismic level required by French nuclear practise (RFS 2001/01 [4]). In this event it shall be demonstrated that all safety functions are maintained. For ITER site the SL-2 (also called SSE – Safe Shutdown Earthquake) Design Response Spectra (DRS) is defined by two spectra: SMS and PALEO spectra. Both types of spectra (or the envelope) need to be analysed.

SMHV (Séismes Maximaux Historiquement Vraisemblables = Maximum Historically Probable Earthquakes) is the most penalising earthquakes liable to occur over a period of about 1000 years [4, 7]

SL-1 corresponds to an event with a probability in the order of 10^{-2} per year and represents an investment protection earthquake level (following the Nuclear Pressure Equipment regulation it corresponds to a foreseeable event). The facility has to be designed to restart and operate after an SL-1 event without special maintenance or test. As this event has a return period of more than 100 years it is expected to occur only once in the machine life. If required by investment protections and the sake of project risk reduction, SL-1 event shall be assumed to occur a maximum number of 5 times because, otherwise, no further operation may be allowed after its occurrence without the additional demonstration that the plan has not degraded the safety level of operation.

The Classification for the seismic conditions is:

SL-2:	Category IV (Extremely Unlikely)
SMHV:	Category III (very Unlikely)
SL-1:	Category II (Likely Event)

For non-seismic class (NSC) buildings [3] the seismic requirement is defined by Eurocode 8 [37] and associated French Order [38].

7.1.1.1 Design response spectra for SC1 and 2 building and equipment

Vertical design soil spectra are assumed to be equal to 2/3 of the horizontal [4] . PALEO spectrum is more severe at low frequencies (for the tokamak complex that is standing on seismic isolators it is generally more relevant for horizontal excitations), while SMS spectrum is more severe at high frequencies (generally, it is more relevant for vertical excitations).

For rock soil[3] the two ground SL-2 DRS PALEO and SMS are shown in fig.7-1.

Fig.6-2 shows the SL-2 DRS obtained by the envelope of SMS and PALEO for different damping values.

Tables 7-1, 7-2, and 7-3 report the values of the acceleration for the two DRS (PALEO and SMS) and for the resulting envelope for different critical damping values.

PALEO and SMS Zero Period Acceleration (ZPA) values are 0.28g and 0.315g respectively (g is the gravity acceleration = 9.81 m/s^2).

SMHV spectra are represented in fig. 7-3. Table 7-4 reports the values of acceleration for the DRS for different critical damping values. Unless a complete SMHV analysis is performed, as a first approximation, seismic response to SMHV event may be obtained multiplying the results from SL-2 by a factor 0.73. The ration between SMHV and SL-2 spectra is not constant at all frequency as shown in table 7.4b and Fig. 7.3b. The factor 0.73 represents the highest value and it is reached at frequency around 11 Hz.

SL-1 seismic level is defined as ¼ of the envelope of the SMS and the PALEO earthquake. So it has a maximum ZPA value of 0.08g [5] . Unless a specific SL-1 analysis is performed, seismic response to SL-1 event may be obtained dividing the results from SL-2 by a factor 3 (factor 3 instead of 4 is used because of the different damping used see par 7.1.1.4).

The Cadarache soil properties are defined in [6]. The soil where the ITER machine is built is classified as rock soil.

Seismic analyses have to be performed considering the uncertainty or variation of the shear modulus G between the minimum value of G/1.5 (soil minoreé) and a maximum of 1.5 G (soil majoreé)[8].

The basemat of the ITER building is seismically isolated from the ground. The properties of the isolation are:

- Partial horizontal FREQUENCY = 0.55 Hz
- Damping ratio in the isolation: 5%

As for the soil properties, a range of variation of the seismic pads stiffness has to be considered to take into account data uncertainty and aging effects [9].

[3] Rock soil is where velocity of S-wave in the first 30m of soil are above 800 m/s according to RFS 2001-01

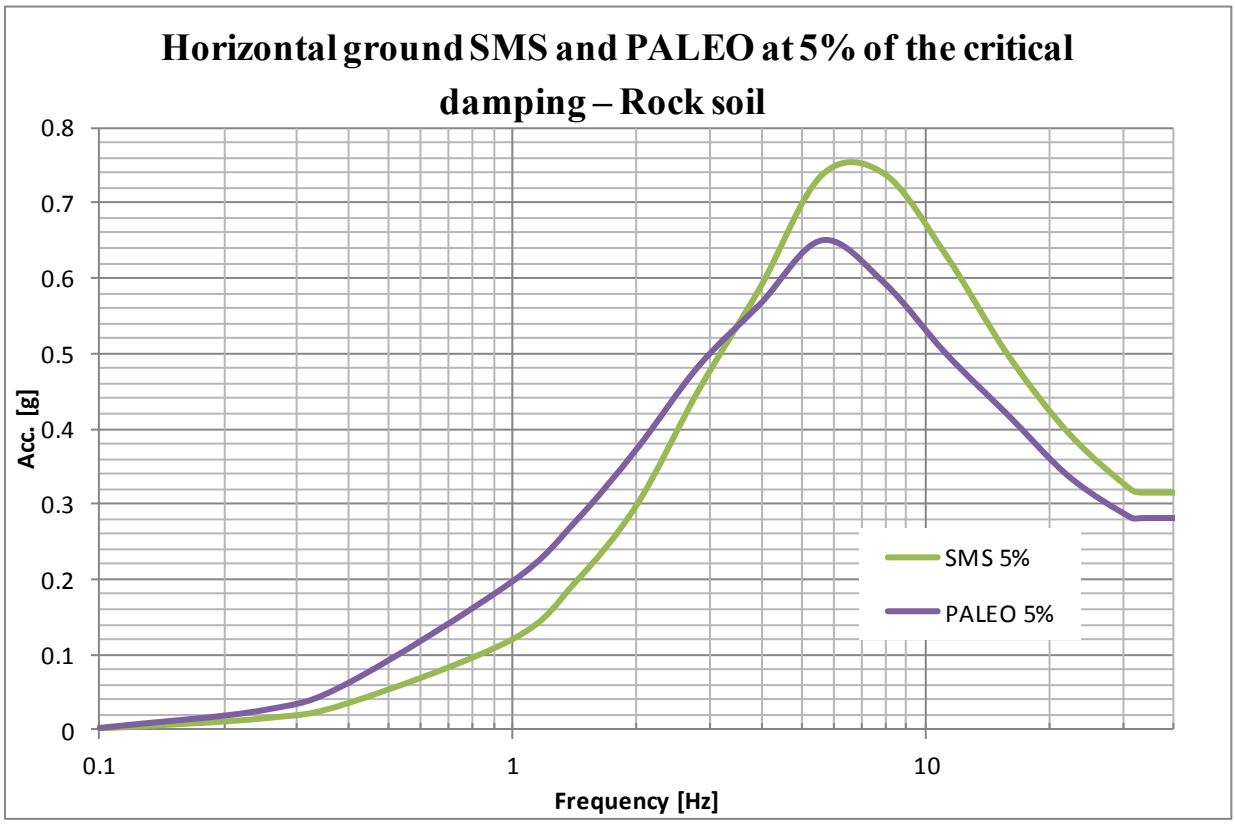

Figure 7-1: Comparison of horizontal ground SL-2 DRS PALEO and SMS at 5% of the critical damping – Rock soil

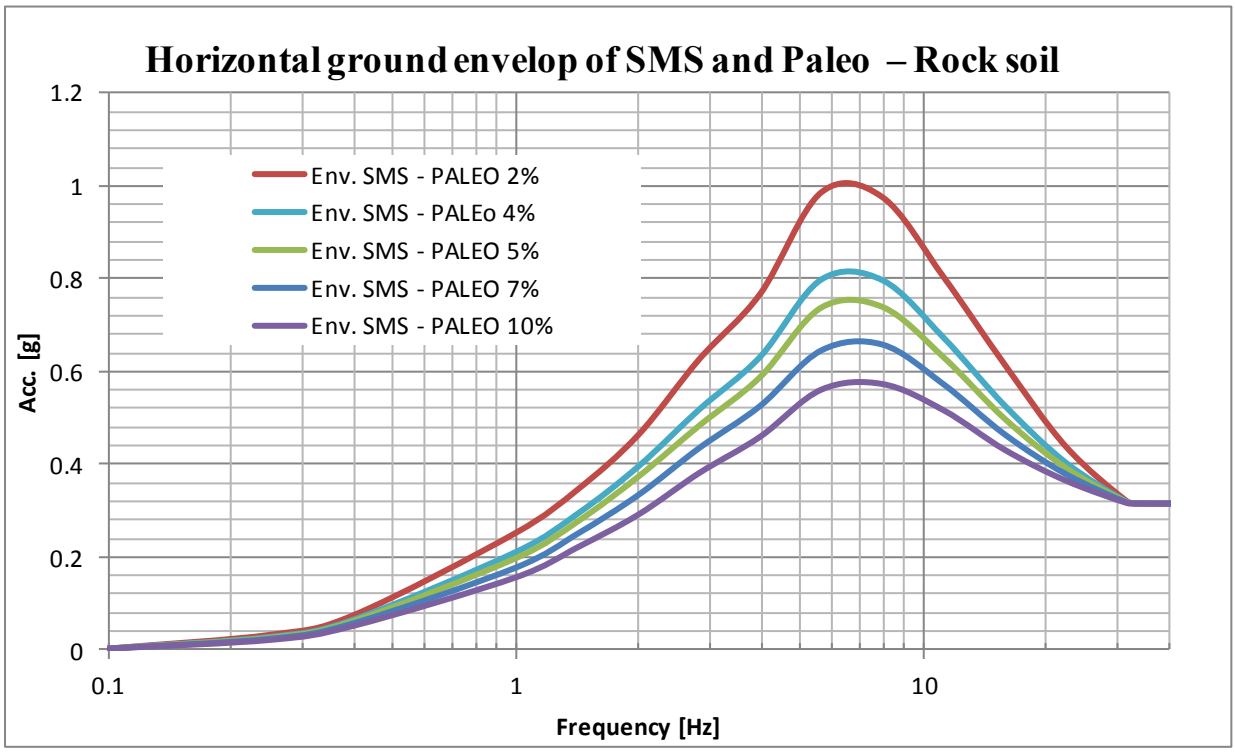

Figure 7-2: Horizontal ground SL-2 DRS (Envelope of PALEO and SMS) for different damping values – Rock soil[4]

[4] The acceleration values for SMS- PALEO at 4% of damping have been calculate from the acceleration values at 2% and 5% by interpolation between spectral amplitude values and natural logarithm of damping ratio. The relation is:

$$\frac{a_{2\%} - a_{4\%}}{a_{2\%} - a_{5\%}} = \frac{ln\frac{2}{4}}{ln\frac{2}{5}} \quad \text{-----} \rightarrow \quad a_{4\%} = a_{2\%} - (a_{2\%} - a_{5\%}) \frac{ln\frac{2}{4}}{ln\frac{2}{5}}$$

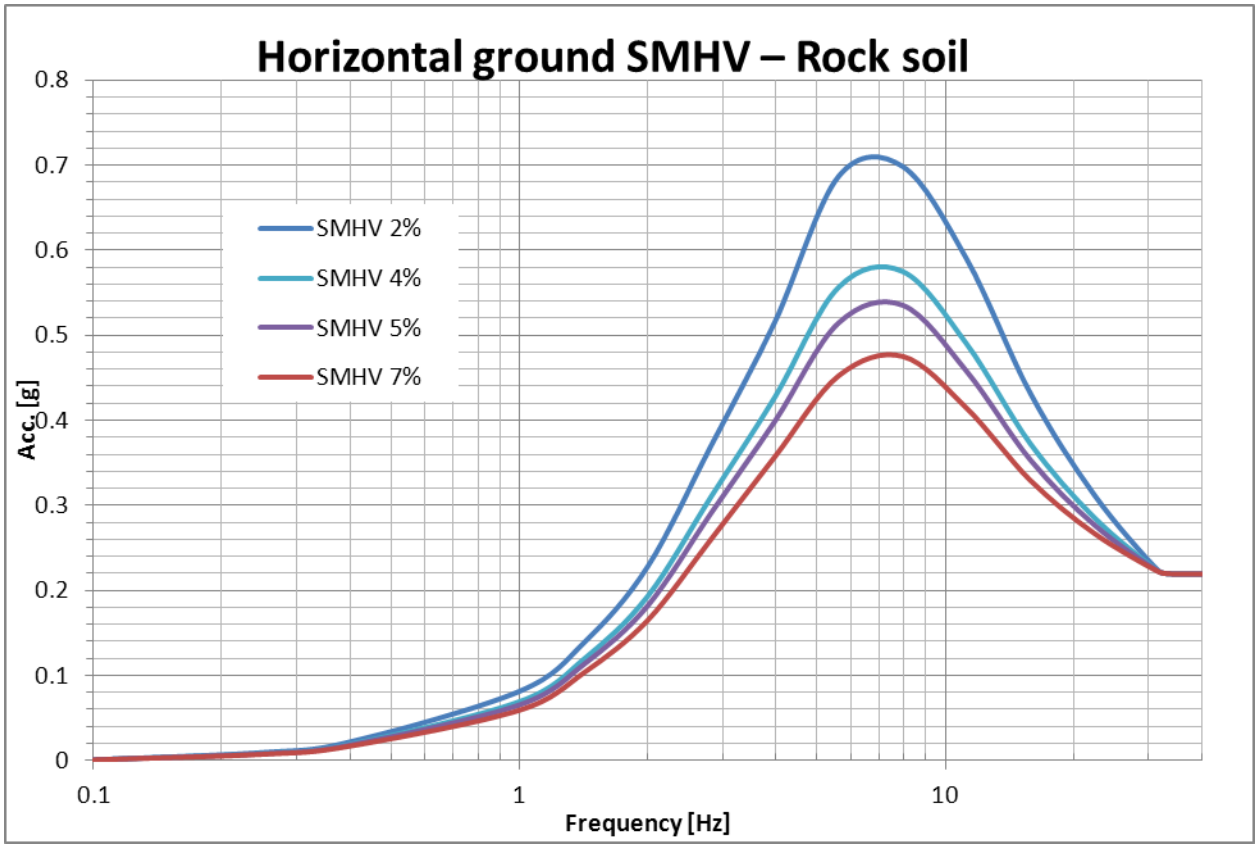

Figure 7-3: Horizontal ground SMHV DRS for different damping values – Rock soil

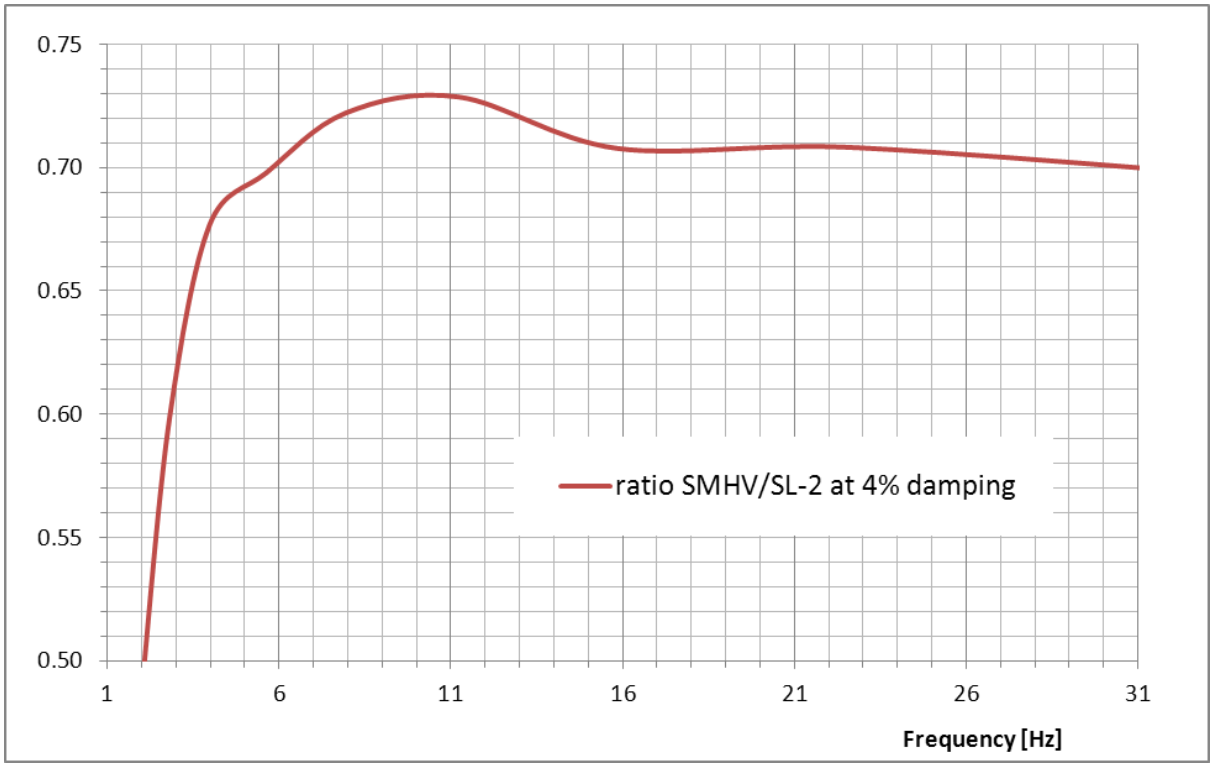

Figure 7-3b: Ratio between SMHV and SL-2 soil spectra at 4% damping value – Rock soil

Table 7-1: SL-2 PALEO DRS horizontal acceleration (in g) – Rock soil

	% of critical damping				
Freq (Hz)	2%	5%	7%	10%	20%
0.1	0.0023	0.0023	0.0023	0.0023	0.0023
0.25	0.0321	0.026	0.0236	0.0211	0.0163
0.4	0.0743	0.0619	0.057	0.0515	0.0398
1	0.2517	0.1971	0.1768	0.1558	0.118
1.42	0.3455	0.2765	0.2502	0.2209	0.1632
2	0.4831	0.3731	0.3335	0.2912	0.2164
2.82	0.6259	0.4829	0.4346	0.3808	0.2814
3.98	0.743	0.5657	0.4995	0.44	0.3337
5.62	0.8807	0.6503	0.5788	0.4952	0.3649
7.94	0.7967	0.5939	0.5252	0.4664	0.3668
11.22	0.6351	0.4995	0.459	0.419	0.3469
15.84	0.5133	0.4181	0.3901	0.3638	0.3213
22.38	0.3661	0.3352	0.325	0.3141	0.2938
31.62	0.2838	0.2812	0.2812	0.2612	0.2812
34	0.2812	0.2812	0.2812	0.2812	0.2812
100	0.2812	0.2812	0.2812	0.2812	0.2812

Table 7-2: SL-2 SMS DRS horizontal acceleration (in g) – Rock soil

	% of critical damping				
Freq (Hz)	2%	5%	7%	10%	20%
0.1	0.0013	0.0013	0.0013	0.0012	0.0012
0.25	0.0183	0.015	0.0137	0.0122	0.0095
0.4	0.0421	0.0352	0.0326	0.0295	0.0232
1	0.1516	0.1201	0.1081	0.0963	0.0757
1.42	0.2406	0.1959	0.1786	0.1588	0.1196
2	0.3782	0.2988	0.2698	0.2381	0.1804
2.82	0.5743	0.4507	0.4039	0.3544	0.2629
3.98	0.7669	0.5877	0.5254	0.459	0.3422
5.62	0.9856	0.7373	0.645	0.5604	0.4083
7.94	0.9754	0.7388	0.6576	0.5726	0.4348
11.22	0.8032	0.6303	0.572	0.5161	0.4157
15.84	0.6148	0.4979	0.4641	0.4309	0.3756
22.38	0.438	0.392	0.3785	0.3644	0.3386
31.62	0.3198	0.3181	0.3172	0.3161	0.315
34	0.315	0.315	0.315	0.315	0.315
100	0.315	0.315	0.315	0.315	0.315

Table 7-3: SL-2 DRS horizontal acceleration (in g) – Envelope of SMS and PALEO – Rock soil

	% of critical damping						
Freq (Hz)	0.5%	2%	5%	7%	10%	20%	30%
0.1	0.0023	0.0023	0.0023	0.0023	0.0023	0.0023	0.0023
0.25	0.0413	0.0321	0.026	0.0236	0.0211	0.0163	0.0141
0.4	0.0931	0.0743	0.0619	0.057	0.0515	0.0398	0.033
1	0.3343	0.2517	0.1971	0.1768	0.1558	0.118	0.0976
1.42	0.4499	0.3455	0.2765	0.2502	0.2209	0.1632	0.1341
2	0.6495	0.4831	0.3731	0.3335	0.2912	0.2164	0.1791
2.82	0.8423	0.6259	0.4829	0.4346	0.3808	0.2814	0.2314
3.98	1.0380	0.7669	0.5877	0.5254	0.459	0.3422	0.2795
5.62	1.3613	0.9856	0.7373	0.645	0.5604	0.4083	0.336
7.94	1.3334	0.9754	0.7388	0.6576	0.5726	0.4348	0.3658
11.22	1.0648	0.8032	0.6303	0.572	0.5161	0.4157	0.3653
15.84	0.7917	0.6148	0.4979	0.4641	0.4309	0.3756	0.3451
22.38	0.5076	0.438	0.392	0.3785	0.3644	0.3386	0.324
31.62	0.3224	0.3198	0.3181	0.3172	0.3161	0.315	0.315
34	0.3150	0.315	0.315	0.315	0.315	0.315	0.315
100	0.3150	0.315	0.315	0.315	0.315	0.315	0.315

Table 7-4: SMHV DRS horizontal acceleration (in g) – Rock soil

	% of critical damping					
Freq (Hz)	0.5%	2%	5%	7%	10%	20%
0.1	0.0006	0.0006	0.0006	0.0006	0.0006	0.0006
0.25	0.0117	0.0094	0.0079	0.0072	0.0064	0.005
0.4	0.0271	0.0217	0.0181	0.0168	0.0152	0.012
1	0.1053	0.0812	0.0653	0.059	0.053	0.042
1.42	0.1772	0.1388	0.1134	0.1035	0.0923	0.0702
2	0.2975	0.2278	0.1817	0.1647	0.146	0.1115
2.82	0.4903	0.3703	0.291	0.2603	0.2287	0.1695
3.98	0.6927	0.5158	0.3989	0.3573	0.3117	0.2302
5.62	0.9479	0.6871	0.5147	0.4525	0.3926	0.2852
7.94	0.9455	0.6986	0.5354	0.4753	0.413	0.3103
11.22	0.7898	0.5899	0.4578	0.4144	0.3722	0.2969
15.84	0.5503	0.4318	0.3535	0.3294	0.3059	0.2658
22.38	0.3657	0.3123	0.277	0.267	0.2568	0.2383
31.62	0.2241	0.2232	0.2226	0.2221	0.2215	0.2194
34	0.2194	0.2194	0.2194	0.2194	0.2194	0.2194
100	0.2194	0.2194	0.2194	0.2194	0.2194	0.2194

Table 7-4b: Ratio between SMHV and SL-2 soil spectra at different frequency and damping values – Rock soil

	% of critical damping					
Freq [Hz]	0.50%	2%	4%	5%	7%	10%
0.1	0.26	0.26	0.26	0.26	0.26	0.26
0.25	0.28	0.29	0.30	0.30	0.31	0.30
0.4	0.29	0.29	0.29	0.29	0.29	0.30
1	0.31	0.32	0.33	0.33	0.33	0.34
1.42	0.39	0.40	0.41	0.41	0.41	0.42
2	0.50	0.49	0.49	0.49	0.49	0.50
2.82	0.58	0.59	0.60	0.60	0.60	0.60
3.98	0.67	0.67	0.68	0.68	0.68	0.68
5.62	0.70	0.70	0.70	0.70	0.70	0.70
7.94	0.71	0.72	0.72	0.72	0.72	0.72
11.22	0.74	0.73	0.73	0.73	0.72	0.72
15.84	0.70	0.70	0.71	0.71	0.71	0.71
22.38	0.72	0.71	0.71	0.71	0.71	0.70
31.62	0.70	0.70	0.70	0.70	0.70	0.70
34	0.70	0.70	0.70	0.70	0.70	0.70
100	0.70	0.70	0.70	0.70	0.70	0.70
Max	0.74	0.73	0.73	0.73	0.72	0.72

7.1.1.2 Rocking effect due to surface wave propagation

Standard seismic analysis considers only translational (vertical and horizontal) motion of a free soil surface as an input excitation.

As the size of the Tokamak Complex building is comparable to the seismic excitation wavelength, appropriated Soil-Structure Interaction shall be considered in particular regarding incoherent (or non-uniform) vertical and horizontal movements at the base of the building. This incoherence can be also influenced by the building embedment.

7.1.1.3 Multi DOF systems

For multi-degree-of-freedom systems, the concept of response spectrum can also be used in most cases by extracting the normal vibration modes and combining them with a modal superposition method.

This consists in transforming the system of differential equations of motion for the multiple-DOF system into a set of independent differential equations and superimposing the results to obtain the solution of the original system.

Thus, the modal superposition method reduces the problem of finding the response of a multi-degree-of-freedom system to the determination of the response of single-degree-of-freedom systems.

An upper limit for the maximum response may be obtained by adding the absolute values of the maximum modal contribution. Generally the results obtained by this method will overestimate the maximum response. Another estimate of the maximum response, which is widely accepted and which gives usually reasonable results, is the Square Root of the Sum of the Squared values of the modal contribution (SRSS method).

However, when some of the modes are closely spaced, the use of the SRSS method can be optimistic. Following the NRC Recommendation [10] the absolute value summation has been considered only for closely spaced modes, which are those with frequencies differing by 10% or less.

7.1.1.4 Damping

In damping, the energy of the vibrating system is dissipated by various mechanisms. In materials, these include plasticity, thermal effects of repeated elastic straining, and internal friction. In structures other effects can contribute even more to energy absorption such as friction at mechanical connections.

For analysis convenience damping is generally assumed to be viscous in nature.

7.1.1.4.1 Damping values for the ITER nuclear building

For the analysis of the nuclear building, the damping vales for seismic level SL-2 are defined in [32]. For SMHV the same damping values as for SL-2 are used.

These values are based on appendix 1 of document [8].

Table 7-5: Damping values for seismic analysis of nuclear building

	SMHV and SL-2
Soil	5%
Seismic isolator	5%
Reinforced concrete	7%
Pre-stressed Concrete	5%
Civil construction bolted steel	7%
Civil constructions welded steel	4%

7.1.1.4.2 Damping values for equipment inside the building

For components and equipment inside the building the damping values are derived from [11]. Damping values are defined for different systems (piping, electrical distribution systems, heating, ventilation and air conditioning ducts, mechanical and electrical components). Table 7-6 reports some data. It is recommended to consult [11] for the implementation into the analyses.

These damping values are intended for elastic seismic analysis where energy dissipation is approximated by viscous damping (i.e., proportional to velocity). The specified SMHV and SL-2 damping coefficient values, for use with elastic analysis, take into consideration the fact that some energy dissipation occurs due to inelastic structural response. Consequently, the specified damping values are not applicable to analyses that explicitly include this inelastic structural behaviour (i.e. material plasticity). In this case the damping value of SL-1 shall be use also for seismic analyses at seismic level SMHV or SL-2.

Table 7-6: Damping factors for seismic analysis

System		SL-1	SMHV and SL-2
General	Welded steel or bolted steel with friction connection	3%	4%
	Bolted steel with bearing connection	5%	7%
Piping	Piping System	3%	4%
Electrical distribution	Cable tray System - Maximum Cable loading	7%	10%
	Cable tray System - Empty	5%	7%
	Conduit System - Maximum Fill	5%	7%
	Conduit System - Empty	3%	5%
Mechanical and electrical components	Motors, Fans, protection housings	2%	3%
	Pressure vessels, Heat exchangers, Pumps and Valves Bodies	2%	3%
	Electrical Cabinets, Panels, Motor Control Centers	2%	3%
	Metal Atmospheric Storage Tanks (containment, protection) - Impulsive Mode	2%	3%
	Metal Atmospheric Storage Tanks (containment, protection) - Sloshing Mode	0.5%	0.5%

7.1.1.4.3 Damping value for the tokamak seismic analysis

The main tokamak components (magnets, VV, in-vessel components, cryostat) are welded structures connected by bolts. The global seismic analyses of the tokamak machine are performed assuming the damping values as defined in table 7-7.

Table 7-7: Damping values for the global tokamak seismic analysis

	SL-1	SMHV and SL-2
Tokamak global seismic analyses	3%	4%

7.1.1.5 Design response spectra for NSC building and equipment

The Design Spectra for non-seismic class buildings are defined following the rules described in Eurocode 8 [37] and associated French Order [38].

7.1.2 Seismic analysis for equipment inside the buildings

Equipment inside the building may or may not have an impact on the building response or the response at the equipment support depending on the equipment mass and natural frequency.

Equipment are defined decoupled from the building in relation to the seismic dynamic response, when one of the following criteria are satisfied [8]:

- Rm < 0.01,
- Rm < 0.10 and Rf > 1.25,
- Rm < 0.10 and Rf < 0.80,

Where Rm represents the ratio between the equipment mass and the mass of the load-bearing structure (building, floor or wall elements), and Rf is the ratio between the fundamental frequency of the carried mass and one of the main frequencies of the load-bearing structure.

If these criteria are not respected, the equipment is defined coupled to the building.

7.1.2.1 Seismic analysis of decoupled equipment inside the buildings

The seismic response of equipment inside the building having a small mass with respect to the mass of the load-bearing structure (building, floor or wall elements), do not affect the seismic response of the building. In this case the equipment are considered decoupled from the building and their analysis can be performed following a two steps approach:

- In the first step the building analysis is performed and the building response spectra are evaluated at different floors (FRS) and locations. In this analysis the equipment masses are included in the model as distributed masses, but there is no need of a proper detailing of the equipment dynamic behavior.
- In the second step the detail analysis of the equipment is performed using as input the FRS at the supports derived from the first step analysis.

Floor response spectra integrate uncertainties related to the modelling of the soil and structure, as well as the variability in the material properties. The variability in ground mechanical properties is taken into account by defining a range of possible variation of soil and isolation pads properties and enveloping the results. Following the smoothing of the transferred spectra, uncertainties related to the structure's characteristics are taken into account by ensuring a minimum frequency broadening of 15% on each side of the spectrum peaks.

The FRS for the design of the equipment in the tokamak, tritium and diagnostic buildings are provided in [27]. This document is based on a well-developed design of building and equipment. Nevertheless reconciliation will need to be performed for the as-built configuration to confirm the adequacy of the calculations and design.

FRS for the Hot Cell Facility, Rad Waste , and Personnel Access Control Buildings are in [28], [29], and [30] respectively. It has to be taken into consideration that the FRS provided in the present version of documents [28], [29], and [30] are based on a very preliminary design of buildings and equipment. It is expected that these FRS will be modified in the future. The user of these spectra has to take precaution in using them (e.g. by adding appropriate margins in the FRS or in the analysis methodology) and to allow contingency for an update of calculation and design.

The floor response spectra are provided for specific values of damping. If for a specific damping value the spectrum is not provided, values can be derived by interpolation using the formula:

$$(A_{i-1} - A_i)/ (A_{i-1} - A_{i+1}) = \ln(\zeta_{i-1}/\zeta_i)/ \ln(\zeta_{i-1}/\zeta_{i+1})$$

$$\rightarrow \; A_i = A_{i-1} - (A_{i-1} - A_{i+1})* \; \ln(\zeta_{i-1}/\zeta_i)/ \ln(\zeta_{i-1}/\zeta_{i+1})$$

A_{i-1}, A_i, and A_{i+1} are the spectral acceleration for the damping value ζ_{i-1}, ζ_i, and ζ_{i+1}.

7.1.2.2 Seismic analysis of coupled equipment inside the buildings

If the mass of any equipment is significant in relation to the mass of the load-bearing structure in question (building, floor or wall element), the risk of coupling between the load-bearing structure and the equipment needs to be taken into account (see criteria in 7.1.2).

When equipment is not considered decoupled in relation to the seismic dynamic behaviour, a global model of the load-bearing structure and the equipment in question is used, thus making it possible to characterize dynamic coupling phenomena.

This is the case for the tokamak machine whose total mass is much smaller than the overall tokamak complex, but is comparable to the mass load bearing structure (tokamak supports and part of basemat).

In this case the seismic analysis of the building has to include a model of the tokamak main dynamic characteristics in order to properly assess the dynamic response at the tokamak support.

Reference [42] reports the seismic analysis of the main tokamak components. This analysis is performed using the two steps approach where FRS at the tokamak supports are obtained from the seismic analysis of the tokamak building which include a simplified model of the main tokamak components. This approach is demonstrated to be conservative as it takes into account uncertainties related to structure's characteristics by frequency broadening.

A single step approach for coupled equipment may be performed. In this approach the analysis model shall include the building main dynamic characteristics and the details of the tokamak. A proper procedure has to be defined to include measures to compensate the uncertainties in the structure's characteristic as in the two steps approach (see 7.1.2.1). It is deemed acceptable to replace the broadening of the floor response spectra that covers the previously defined uncertainty by a series of spectra.

7.1.2.3 Seismic analysis of components attached to the tokamak

Many equipment are attached to (or supported by) the tokamak main components (magnet, VV, cryostat, etc.). These equipment, that have a small mass with respect to the main components, may not be modeled in details in the global tokamak analysis (only distributed masses are included). As they are decoupled from the main tokamak components, their behaviour does not significantly alter the seismic behavior of the main tokamak components to which they are attached, but their seismic response may be very different.

To perform the detail seismic analysis of these equipment the definition of the seismic excitation at the support points is needed. The analysis procedure can be similar to the response spectra method adopted for the equipment in the building.

Point Response Spectra (PRS = Spectra calculated at specific points of the supporting structure)[5] may be used for Spectrum Seismic Analysis of comparatively small-mass equipment, which was not included into the global finite-element model.

The classic method to obtain Response Spectra is based on time-history analysis. However, this method is extremely time-consuming. As the input accelerograms are often only available at the free soil surface, the PRS from direct time-history analysis may be obtained in case single step analyses are performed for the tokamak as described in 7.1.2.2.

In alternative, the so-called direct method "from spectrum to spectrum" may be used. Several direct methods are described in literature and mentioned in ASCE 4-98 [44] and ASME Appendix N [45].

Reference [42] reports the PRS at several locations on the Cryostat, Magnets and VV.

[5] Other synonym names are "In-Structure Spectra" and "Secondary Spectra"

7.1.2.4 Modelling of liquids

Recommendation for seismic analysis of tanks and container filled by liquids are provided in section 2.4.6 of [8].

To calculate seismic loads applied to the walls of tanks and pools, the contained liquid masses are represented in modelling.

The analysis procedure shall take into account impulsive actions (action of fluid moving rigidly with the container boundaries) and convective (sloshing) actions (actions of the liquid moving in long-period sloshing motion) of the liquid in flexible steel or concrete tanks fixed to rigid foundations.

Simplified analysis procedure as proposed by Eurocode 8 (Part 4: Silos, tanks and pipelines) [43] may be followed.

7.2 Plasma current disruptions

A general top-level characterization of plasma scenarios and disruptions is contained in section 4.3 of the PR document [1]. Table 4.1 of PR document gives plasma reference scenarios with the highest of fusion power and the plasma current being 500MW and 15 MA, respectively. In chapter 4.3.1.3 PR document defines additional “flexible scenario” with:

- D-T plasma scenarios with up to 700 MW of fusion power for 100 s;
- D-T plasma scenarios with plasma currents of up to 17 MA.

These flexible scenarios should not lead to additional technical requirements for the ITER systems and structures with respect to those derived from the D-T reference plasma scenarios, except for the magnet that shall be designed to operate at 17 MA plasma current.

The impact on VV of 700 MW fusion power for 100 s shall be evaluated: it shall be demonstrated that temperatures and stresses in VV shall be enveloped by the 500 MW for 450 s scenario.

The scenario with plasma current up to 17 MA will be allowed for plasma configurations having demonstrated during the progressive approach to high machine performance ("Progressive Start-up" strategy as per the RPrS [22]) that VV and in-vessel components loads are not larger than the design values obtained from 15 MA with the conservative assumptions on halo and eddy currents loads. For this reason only the disruption and halo EM loads from the 15 MA plasma scenario are considered for the design of the ITER components.

The following paragraphs extend the details of this classification for EM and structural modelling purposes.

A summary of the design specifications for the disruption cases is reported in the table A-1.1 and A-1.2 of Appendix A.

A plasma disruption is characterised by two phases:

- thermal quench;
- current quench.

Based on the current quench shape, the heat load transferred to the plasma facing structures, and the amount of runaway electrons generated by the disruptions are classified into four types: I, II, III, and IV.

In disruptions faster current decays give origin to the larger eddy currents. In case of slow_fast current decay (see description in 6.2) the disruption could evolve in vertical plasma instability (cold VDE). This may have, as a consequence, similar level of the induced eddy currents for the in-vessel components, together with an increase of halo current loads. As the fast plasma current decay generates larger (or equal) eddy current loads than slow_fast transients and halo

current in VDEs are larger than halo current in cold VDEs that follow a slow_fast disruption, the slow_fast disruption loads are considered enveloped by the mentioned events. It is anyway defined an extreme slow_fast disruption that is classified in load category IV that needs to be considered for the design of the ITER components.

Plasma current disruptions induce loads that are generally of limited time duration and vary in a time range that is comparable to the natural periods of the structures. For this reason, the dynamic effects need to be taken into account.

The energy of the vibrating system is dissipated by various mechanisms. The major contribution is generally provided by small material plasticity and friction at mechanical connections. For analysis convenience damping is generally assumed to be viscous in nature.

The recommended damping values to be assumed in dynamic analyses of plasma transient events are defined in Appendix II.

7.2.1 Thermal quench

The thermal quench is triggered by the onset of a plasma instability that drives a sudden loss of confinement introducing chaotic perturbations in the plasma nested magnetic configurations and thus largely increasing the radial (normal to the magnetic field lines) energy transport contribution that is normally very low. The thermal quench produces a very fast increase of the toroidal flux (in ≅ 1 ms time, comparable to the onset time of the instability that has driven the thermal quench). This field variation is due to the decrease of the plasma diamagnetism associated with the gyration velocity of the electrons around the field lines; the MHD instability induces the current flattening in a sub-millisecond time scale, which is much shorter than the current diffusion time for ITER (even in the cold plasma), which is in the range of some tens of ms. The decay of plasma diamagnetism induces *skin* poloidal currents in the first wall component (as close as possible to the plasma) and in the VV aiming to preserve the toroidal flux; at the same time, after the beta decay, the external field, that is now larger than the value needed for the equilibrium, shrinks the plasma inducing a fast inward movement of the plasma centre. As a consequence of this movement a poloidal field variation can occur in the in-vessel components. Due to the very fast time rate of this phenomenon the EM loads observed in this phase are, for some components, of the same order of magnitude of the loads driven by the plasma current quench where a much higher but slower poloidal field variation occurs. The current quench follows the thermal quench as a consequence of the large increase in plasma resistivity.

A summary of the thermal quench specifications is reported in table A-1.2.

7.2.2 Disruption of Type I (MD I)

This event is expected to be a normal worst case fast disruption.

Two possible plasma current decays are considered:

- Linear with a time duration Δt=50 ms --> $I=I_0(1-t/\Delta t)$
- Exponential with time constant τ=22 ms --> $I=I_0e^{-(t/\tau)}$

The halo current in fast disruption is generally very small. The maximum halo current value is defined by the peak of the product of the toroidal peaking factor (TPF) and the total halo current (Ihalo) divided by the plasma current (Ip) calculated before the thermal quench. This maximum value is TPF*Ihalo/Ip = 0.15.

For the definition of the TPF and the toroidal distribution of halo current see par 7.3.5.1.

The main disruption characteristics are:

Table 7-8: Type I disruption definition

Initial Plasma State	SOF - EOB
Condition category	I: Normal
Initial Plasma current	15 MA
Total duration to zero plasma current	Δt=50 ms and τ=22 ms
Peak TPF*Ihalo/Ip	0.15
Minimum thermal energy quench time [12][13]	3 ms
Expected number of events	2600 (*)

(*) See paragraph 7.2.6

7.2.3 Disruption of Type II (MD II)

This event is expected to be an upset worst case fast disruption.

Two possible plasma current quench decays are considered [14]:

- Linear with a time duration Δt=36 ms --> $I=I_0(1-t/\Delta t)$
- Exponential with time constant τ=16 ms --> $I=I_0e^{-(t/\tau)}$

The main disruption characteristics are:

Table 7-9 : Type II disruption definition

	fast
Plasma movement	Up or down
Initial Plasma State	SOF - EOB
Condition category	II: Likely
Initial Plasma current	15 MA
Total duration to zero plasma current	Δt=36 ms and τ=16 ms
Peak TPF*Ihalo/Ip	0.15
Minimum thermal energy quench time [12][13]	1 ms
Expected number of events (*)	400

(*) See paragraph 7.2.6

The minimum thermal energy quench time is assumed equal to 1 ms.

7.2.4 Disruption of Type III (MD III)

This event is expected to be an emergency worst case fast disruption.

This event is considered in the load specification to take into account fast plasma current quench associated with exceptionally fast plasma thermal quench.

Special pulses performed on some of the presently operating tokamak generated data that extrapolated to ITER give very fast plasma current quench. The probability of these fast quenches in ITER is reasonably low and ITER can be operated by carefully planning and limiting the operational boundary following a learning process of every plasma configuration starting from low plasma currents in order to reduce the probability of these very fast events in high performance plasma scenario. The plasma current quench conditions defined as boundary

for disruption type II represent a physical limit for the machine. For this reason the disruption type III events have the same current quench specification as disruption type II.

With respect to MDII a faster thermal energy quench is assumed with a minimum time duration equal to 0.5 ms.

Two possible plasma current quench decays are considered:

- Linear with a time duration Δt=36 ms --> $I=I_0(1-t/\Delta t)$
- Exponential with time constant τ=16 ms --> $I=I_0e^{-(t/\tau)}$

The main disruption characteristics are:

Table 7-10 : Type III disruption definition

Initial Plasma State	SOF - EOB
Condition category	III: Unlikely
Initial Plasma current	15 MA
Total duration to zero plasma current	Δt=36 ms and τ=16 ms
Peak TPF*Ihalo/Ip	0.15
Minimum thermal energy quench time [12][13]	0.5 ms
Expected number of events	-

7.2.5 Disruption of Type IV (MD IV)

This event is considered in the load specification to take into account extremely fast and slow_fast plasma current quench.

Disruption current quench time has been defined based on a statistic database from running machines obtained excluding events with plasma configurations that are not ITER relevant. As a measure of safety protection the excluded data points from the statistic have been used to define an extremely unlikely fast disruption event (MD IV).

The thermal energy quench time is assumed equal to 0.5 ms.

Two possible plasma current quench decays are considered:

- Linear with a time duration Δt=26 ms --> $I=I_0(1-t/\Delta t)$
- Exponential with time constant τ=11.3 ms --> $I=I_0e^{-(t/\tau)}$

The main disruption characteristics are:

Table 7-11 : Type IV disruption definition

	Fast	Slow_fast	
	Up or down	Up	Down
Initial Plasma State	SOF - EOB	SOF - EOB	
Condition category	IV: Extremely unlikely	IV: Extremely unlikely	
Initial Plasma current	15 MA	15 MA	
Total duration to zero plasma current	Δt=26 ms and τ=11.3 ms	(*)	
Peak TPF*Ihalo/Ip	0.15	0.6 (**)	0.75 (**)
Minimum thermal energy quench time [12][13]	0.5 ms	0.5 ms	
Expected number of events	-	-	

(*) Plasma current decay is initially slow, later dIp/dt is the same as MD III fast in linear current decay

(**) As a full characterisation of the slow_fast event is not completed, it can be assumed, conservatively, that the same halo current as in Slow VDE III are applied for upper and lower vertical movements of the plasma

7.2.6 Number of disruption events

For the design of ITER components it is assumed that 10% of the total number of full power pulses will end with a plasma disruption which gives a total number of 3000 disruptions. The experimental data from present fusion devices show that severity of a plasma disruption can vary from case to case.

A statistic distribution for ITER is derived following the most severe disruption statistic among the present running fusion devices. This is provided by DIII-D and is shown in fig.7.2.6-1[15][16]. This figure reports the frequency of current quench time assumed for the design of ITER components.

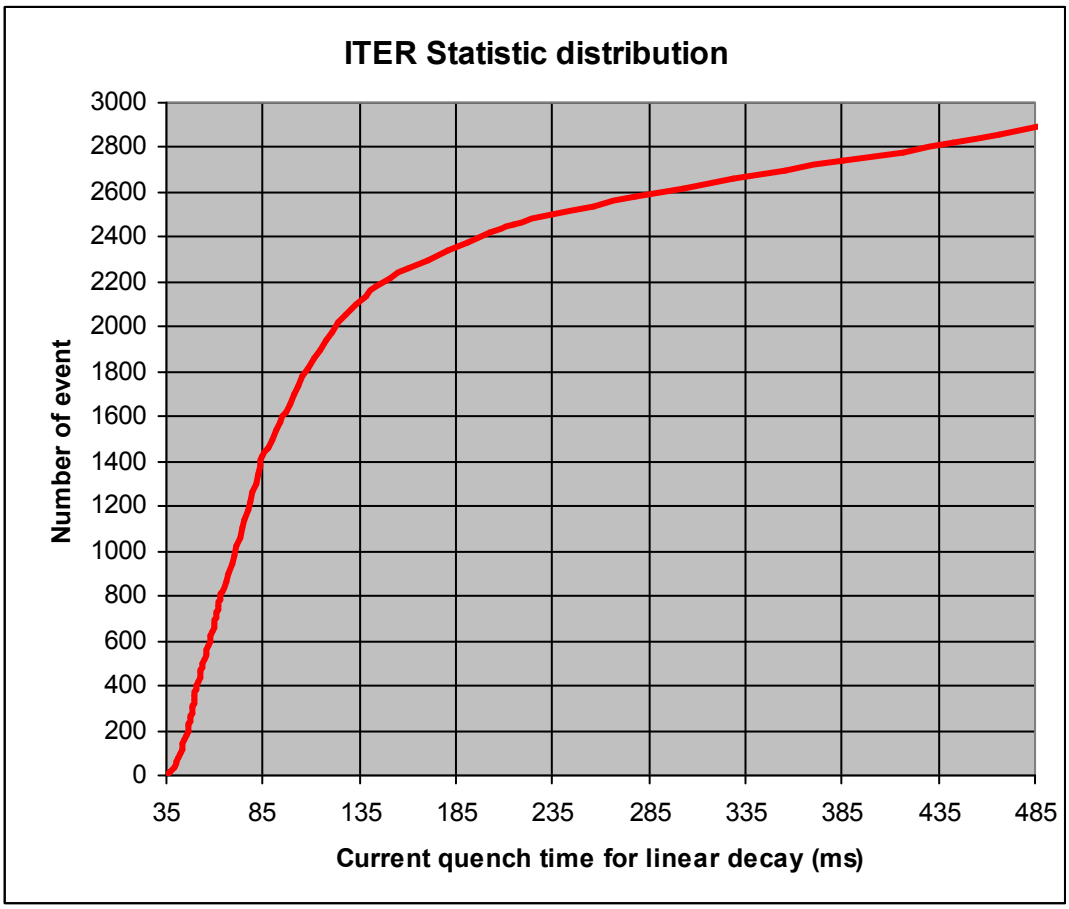

Fig. 7.2.6-1: Frequency of plasma current quench time assumed for the design of ITER components (linear current quench)

Following this distribution, the more severe condition for a MD I event (50 ms and 22 ms for linear and exponential decays) envelopes 87% of all disruptions (2600). The most severe condition for disruption II envelops the rest 13% (400). A summary is reported in table 7-12.

Table 7-12: Frequency and main parameters for ITER fast disruption types I, II, III, and IV

Load case	Units	MD I	MD II	MD III	MD IV
Load category	-	I - Normal	II - Likely	III - Unlikely	IV - Extremely unlikely
Number of events		2600 (*)	400 (*)	-	-
Current quench duration (if Linear decay)	ms	≥50	≥36 <50	36	26
Current quench duration (if Exp decay)	ms	≥22	≥16 <22	16	11.3

(*) For the statistic distribution of the plasma current quench time see fig. 7.2.6-1.

The number of events to be considered for the design has an impact on the fatigue damage and the aging effects.

For the majority of the cases the loads and maximum strains in the structures surrounding the plasma can be assumed, as first approximation, proportional to 1/tcq (tcq=current quench time). In these cases, to simplify the analyses, the total cumulative damage of the full disruption population can be calculated assuming an equivalent number of disruptions with the most extreme condition for disruption II (36 ms linear or 16 ms time constant for exponential) or for disruption I (50 ms linear or 22 ms time constant for exponential). By doing that the number of disruption events that produces the same fatigue damage of the full disruption population is much smaller than 3000.

7.2.7 Runaway electrons

During the plasma current quench large induced electric fields are generated. These can accelerate the electrons to high energy generating runaway electrons (electrons that escape from the plasma core and impact on the first wall).

This phenomenon causes localised energy load to the first wall.

The runaway electron population generates an increase of the plasma current (or better reduces the speed of the plasma current quench). For this reason the runaway electron phenomenon is not associated with fast plasma current quench events.

Specifications for runaway electrons are provided in [2]. Although it is specified in [2] that the runaway electrons are generated for all of the disruption events, EM load analysis should be performed with the conservative assumption that no runaway electrons are generated. This is partially justified by the fact that disruption mitigation system is planned to be installed, with which runaway electrons are suppressed for most of the disruption events.

7.3 Plasma VDEs

In operating the ITER machine a cautious approach will be applied in order to avoid unstable scenarios that can lead to VDEs. For that reason VDEs are not expected to be regular events and can occur only in case of malfunctions of the control system due to excessively large perturbations and for special configurations. Nevertheless, to prevent precluding possible experimental campaign and mode of operations, there are VDEs that have been considered as likely operating conditions.

VDEs of different types can occur during the life of the machine depending on the type of plasma operation and magnetic configuration. To simplify the load definitions the VDEs have been grouped depending on:

- The severity of the loads (typical maximum or type II and worst case or type III)
- The speed of the plasma current quench (fast, slow, and slow_fast)
- The direction of the plasma movement (upward or downward)

A plasma VDE is characterised by three phases:

- start of plasma vertical movement;
- thermal quench;
- current quench.

The worst case VDE or type III VDE represents an extreme worst possible case. It is considered an unlikely event, and it is assumed that it will occur only a few times in the machine life. The typical maximum VDEs or type II VDEs are representative of a larger number of events that are expected to occur more frequently.

Database from the running machine show that in some cases the plasma can enter in a rotating kink mode. The rotating frequency varies in a wide range (up to 1-2 kHz), but in some cases it is very slow and sometimes it locks (after several rotations, it can stop and lock).

When the rotating frequency remains very high, no dynamic amplification is seen by the mechanical structures, but as it come close to one of the natural structural frequency a large dynamic amplification may occur. To cover this condition it is assumed that during the whole current quench phase of the slow VDE the rotation continues at a frequency that provides the maximum dynamic amplification of the response. The probability that this event occurs and that the rotation of the asymmetry perfectly stay synchronised with the natural frequency of the structures in order to generate this large dynamic amplification is considered an extreme event that is classified in category IV.

A summary of the design specifications for the VDE cases is reported in the table A-2 of Appendix A.

7.3.1 Typical maximum VDEs (Type II)

For type II VDEs, the assumption is that they will occur 300 times in the lifetime of the machine. The severity of the halo current for this type of VDEs is defined on a deterministic approach and represents the envelope of the majority of VDEs.

For slow downward VDEs the halo current loads is defined by the formula

$$Ihalo*TPF/Ip = 0.42$$

That corresponds to 56% of the value defined for the corresponding VDE III case. This factor can be used as scaling value for all halo current loads from type III to type II.

The specification of the plasma current quench duration for the fast VDE II are equivalent to those defined for the MD II events. Load due to eddy current is to be evaluated according to the current quench duration specified. Their Category is II.

7.3.2 Worst case VDEs (Type III)

7.3.2.1 Type III slow current quench VDE (VDE/S)

In this worst case scenario:

1. the plasma remains in a healthy (full plasma current) configuration while it is vertically drifting until it becomes a *limiter* plasma
2. The plasma continues to drift vertically without current quench until q_{edge} reaches the critical value of 1.5. At that time a fast thermal quench takes place.
3. Slow current quench disruptions are thought to give rise to higher vertical loads on the passive structure since they allow additional plasma vertical drift into the destabilizing quadrupolar field.
4. Halo currents will develop and will contribute to the global vertical equilibrium. They will start developing as soon as the plasma becomes limiter-like.

The above VDE scenario followed by a slow current quench (VDE/S) can be summarized in the following table [18][19][20]:

Table 7-13: Definition of type III VDE followed by slow current quench

	VDE/S type III	
Initial Plasma State	SOF - EOB	
Condition category	III: Unlikely	
Thermal Quench initiator	q=1.5	
Plasma Current quench duration	≥200 ms	
Direction of movement	Down	Up
Expected number of events	-	
Total maximum halo current [MA] (1) (for downward VDEs)	8.16	6.5
Peak (Ihalo*TPF/Ip) (2) (3)	0.75	0.6
Peak total net horizontal load [MN] (1)(3)(4)	22	48
Maximum total net vertical force [MN] on magnets and VV(1)(3)(4)(5)	108	86

(1) This number have been obtained increasing by a factor 1.2 the data from computer simulation to compensate for uncertainties and envelopes experimental measurements from the statistic database

(2) TPF = Toroidal peaking factor of the halo currents (see par 7.3.5.1)

(3) Value for a downward/upward VDE – see also par. 7.3.6

(4) For the combination of the maximum vertical and horizontal forces see par. 7.3.7.

(5) In downward (upward) VDE maximum applied vertical force on VV is directed downward (upward). PF magnets and VV has equal opposite forces.

The time behaviour of the total vertical force is defined following the 2D simulation provided by the DINA code [26]. VDEs with slower current quench have higher halo current/vertical forces. Maximum duration of the vertical force can be assumed equal to 1-1.5s. A shorter time shall be considered if generates larger dynamic amplification factors.

Time behaviour of the asymmetric loads is provided in [20].

For asymmetric load see par. 7.3.5

7.3.2.2 Type III fast current quench VDE (VDE/F)

The above described Type III VDE/S is particularly severe for the intensity of the net vertical loads and the impact on the Vacuum Vessel.

Experimental observations in operating tokamaks and computer simulations have demonstrated that in case of fast VDEs the severity of halo current and net vertical and horizontal forces reduces considerably.

In a fast VDE the maximum assumed value of the product (Ihalo*TPF/Ip) as well as the net horizontal load are equal to 60% of what is assumed for the VDE/S.

In fast VDEs the forces on the passive structures are generated by combinations of induced eddy and halo currents. Their maximum values can occur at different times.

To take into account the toroidal peaking of the loads, the same TPF assumed for the slow VDE cases is applied to the fast events. For asymmetric load see par. 7.3.5.

Table 7-14: Definition of type III VDE followed by fast current quench

	VDE/F type III	
Initial Plasma State	SOF - EOB	
Condition category	III: Unlikely	
Thermal Quench initiator	q=1.5	
Plasma Current quench duration	as Disrupt type III	
Direction of movement	Down	Up
Expected number of events	-	
Total maximum halo current [MA] (for downward VDEs)	4.9	3.9
Peak (Ihalo*TPF/Ip) (1)	0.45	0.36
Peak total net horizontal load [MN] (2)(3)	17	29
Maximum total net vertical force [MN] on PF magnets and VV (2),(3)(4)(5)	66	50

(1) TPF of the vertical force equal to the value assumed for the slow event

(2) Value for a downward/upward VDE – see also par. 7.3.6

(3) For the combination of the maximum vertical and horizontal forces see par. 7.3.7

(4) Vertical forces are due to induced and halo currents

(5) In downward (upward) VDE maximum applied vertical force on VV is directed downward (upward) – PF magnets and VV has equal opposite forces.

7.3.3 Extreme VDEs (Type IV)

7.3.3.1 Type IV slow_fast current quench VDE (VDE/SF)

Experiments show that there are discharges, which exhibit ‘slow_fast’ type current quench waveforms. In this VDE, the plasma current decays very slowly during the initial quench phase (quench rate similar to Type III slow). At some transition current, I_{trans}, the plasma current starts to decay very fast (similar quench rate of Type III fast).

Large halo and large eddy currents could occur simultaneously, which leads to overlapping of large EM load due to halo and eddy currents. This type of VDE waveforms is categorized as ‘slow_fast’.

ASDEX-Upgrade experimental data show that such transitions occur when edge q value becomes 2, which suggests that MHD activity triggers this transition. However, JET data show no clear dependence on q value. Because the occurring condition of ‘slow_fast’ current quench waveform is not clearly identified, the transition current is specified from the experimental data.

Based on the JET data examinations, transition currents normalized to the pre-disruptive plasma current, I_{trans} / I_{p0} during 'slow_fast' current quench in ITER can be specified in the following range [40]:

$$I_{trans} / I_{p0} \approx 0.75\text{-}0.95$$

Within these ranges, design of support structure should be performed for the transition current, which generates the largest EM load by the combined halo and eddy currents.

To take into account the toroidal peaking of the loads, the same TPF assumed for the slow VDE cases is applied to the slow fast events. For asymmetric load see par. 7.3.5.

Table 7-15: Definition of type IV VDE followed by slow_fast current quench

	VDE/SF type IV	
Initial Plasma State	SOF - EOB	
Condition category	IV: Extremely Unlikely	
Thermal Quench initiator	q=1.5	
Transition currents I_{trans} / I_{p0} from slow to fast current	0.75-0.95	
Plasma Current quench duration (quench rate)	as Disrupt type III	
Direction of movement	Down	Up
Expected number of events	-	
Total maximum halo current [MA]	8.16	6.5
Peak (Ihalo*TPF/Ip) (1)	0.75	0.6
Peak total net horizontal load [MN] (2)(3)	22	48
Maximum total net vertical force [MN] on PF magnets and VV (2),(3)(4)(5)	108	86
(1)TPF of the halo current equal to the value assumed for the slow event (2) Value for a downward/upward VDE – see also par. 7.3.6 (3) For the combination of the maximum vertical and horizontal forces see par. 7.3.7 (4) Vertical forces are due to induced eddy and halo currents (5) In downward (upward) VDE maximum applied vertical force on VV is directed downward (upward) –PF magnets and VV has equal opposite forces.		

7.3.3.2 Type IV rotating asymmetric VDE

The rotation of the plasma halo current asymmetry in VDEs has been observed in present experiments, but a full characterization of this phenomenon has not been completed as experimental observations are very limited. As a safety measure and for investment protection this condition shall, anyway, be taken into account with the most pessimistic assumptions. This event is classified in category IV. During operation ITER will operate following a progressive approach to high machine and plasma performance in order to verify that the specified design conditions are not exceeded.

For the VV and magnet the total asymmetric forces and moments including the time functions evolution and the values in the cases of the rotating kink modes are reported in [20].

Additional specifications and guidelines are provided in Appendix I.

7.3.4 Halo current density and maximum halo current on in-vessel components

The maximum poloidal halo current density calculated at the first wall surface perpendicular to the magnetic poloidal field lines in slow VDE III and VDE II cases are 300 kA/m^2 and 200

kA/m^2, respectively. This value has to be used for the analysis of small part of components. Increase of the local halo current by TPF can be introduced by the increase of the wetted area by the halo plasma due to the increase of halo width.

Design value of the halo current for in-vessel components depends on the poloidal location inside the VV. The estimate of the intercepted halo currents shall include the interception of the poloidal and toroidal components. Table 7-16 and 7-17 define the design value of the intercepted poloidal halo current. Data reported in the table do not represent a single simulation event, but represent envelop of many possible VDE cases.

The value of the intercepted toroidal current depends on the assumed misalignment of the components. A study on the halo current in each blanket module for different plasma simulation is reported in [35]. A further revision of the maximum intercepted halo current by Module 1 is presented in [36].

Table 7-16: Maximum intercepted poloidal halo current in each module in slow VDE III (3)(4).

Blanket Module number	Number of modules in a toroidal row	Toroidal angle of a single module (°)	Plasma VDE direction	Maximum total halo current [MA] (5)	Maximum Intercepted halo current by a single module (kA) (2)
1	18	20	down	8.16	197
2	18	20	Down	8.16	136
3	18	20	Down	8.16	136
4	18	20	Up	6.48	108
5	18	20	Up	6.48	180
6	18	20	Up	6.48	180
7	18	20	Up	6.48	180
8	18	20	Up	6.48	180
9 (1)	18	20	Up	6.48	180
10 (1)	18	15.5	Up	6.48	180
Upper plug (1)	18	4.5	Up	6.48	52
11 (1)	36	10	Up	6.48	90
12	36	10	Up	6.48	36
13 (1)	36	10	Up	6.48	36
14 (1)	18	8.6	Up	6.48	31
15 (1)	18	8.6	Down	8.16	39
Equatorial plug (1)	18	11.4	Down	8.16	103
16 (1)	36	10	Down	8.16	45
17	36	10	Down	8.16	45
18	36	10	down	8.16	180

(1) Port plugs are assumed radially aligned with surrounding blankets. If plugs are radially set back to reduce the halo current, the value in the table needs to be corrected. The correction needs to be applied also to adjacent modules.

(2) TPF is included.

(3) Additional halo current due to misalignment of the blanket modules shall be taken into account. Recommended value for peak factor is equal to 1.15. As this value is design or installation dependent it shall be corrected if design or installation parameters are modified.

(4) Halo current values depend on the design of each blanket module. Values in this table refer to the blanket module design defined in ITER baseline 2011.

(5) This value represents the percentage of total halo current including 20% uncertainty applied to DINA plasma transient simulations

Table 7-17: Maximum intercepted poloidal halo current in divertor components of a single cassette (6.67°) in slow downward VDE III (1)(2)

Component	Max intercepted halo current (kA) (3)
Maximum inlet halo current	146
Inner vertical target	146
Dome	98
Outer vertical target	146

(1) The data for single components in the table refers to envelop values and are not related to a single event. To calculate the maximum support or interface loads a halo current distribution in each component consistent with a single VDE event has to be analysed.

(2) Additional halo current due to misalignment of the divertor cassettes have to be taken into account. Recommended value for peak factor is equal to 1.15. As this value is design or installation dependent it shall be corrected if design or installation parameters are modified.

(3) TPF is included

In case of fast VDEs the maximum values reduce by a factor 0.6.

In VDE II cases the maximum halo current values for the in-vessel components correspond to 56% of the VDE III cases.

7.3.5 Specification of the modelling of non-axisymmetric loads for low q, full blown VDEs

Some experimental results seem to indicate that, in VDEs, non-axisymmetric instabilities (e.g., kink) may develop in the plasma. Evidence of this phenomenon is often seen in the form of a toroidal peaking of halo currents.

The main structural consequences of this event are: 1) a higher local pressure at the first wall, the blanket modules, and the divertor cassettes due to halo currents, and 2) the generation of substantial horizontal forces acting between magnet and passive structure.

7.3.5.1 Halo toroidal peaking factor

The halo current toroidal peaking factor is defined as the ratio between the maximum halo current in one toroidal sector and the toroidal average value. Regarding the toroidal load peaking, the worst case halo current event (VDE_{WC}) corresponds to the type III VDE/S. For this case it is defined that

$$TPF*(Ihalo/Ip) = 0.75$$

This value is taken from the upper boundary of experimental data in various machines. Since computer simulations of VDEs and disruptions (generally 2D) provides only the total halo current and not a local maximum value the TPF for a particular computed total halo current (Ihalo) can be evaluated as:

$$TPF = (0.75 * Ip)/Ihalo$$

Figure 7.3.5-1 shows the bounding curves for the VDE_{WC} (type III) and the VDE_{TM}. The maximum value of the halo current for VDE_{WC} is based on computer simulation performed including the most pessimistic assumptions for the event. For conservatism the calculated halo current number is multiplied by an uncertainty factor 1.2.

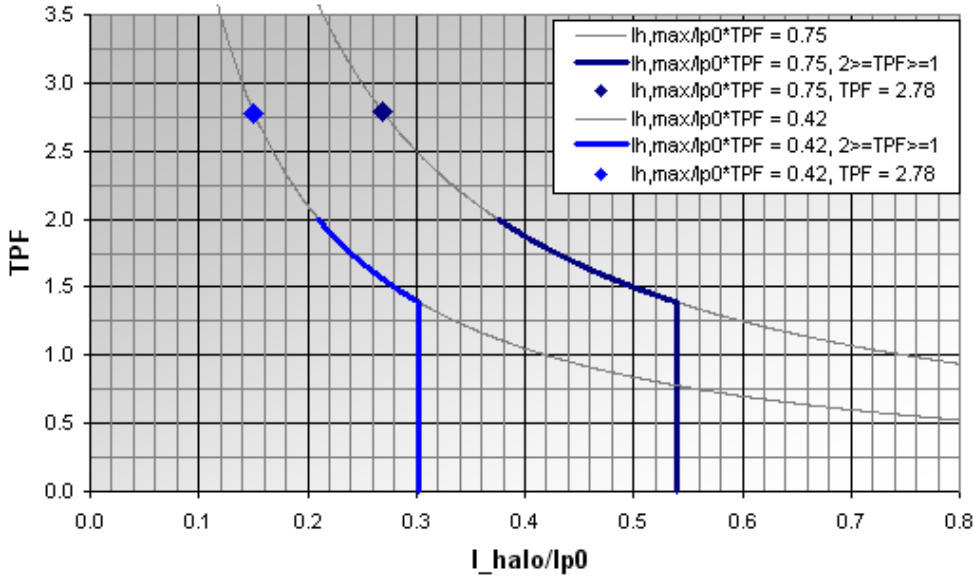

Figure 7.3.5-1: Specification of TPF(I_{halo}/I_p) for VDE_{WC} slow downward (dark blue) and VDE_{TM} slow downward (light blue)

The toroidal asymmetry of the halo and induced currents in plasma surrounding structures can induce not only an exchange of horizontal and vertical forces, but also tilting moments that need to be considered in the design. These forces and moments are typically exchanged between the VV and the magnets.

7.3.5.2 Horizontal load and toroidal distribution

The TPF is defined to take into account the toroidal variation of the halo current intensity. In general, the above definition is not sufficient to obtain the net horizontal load between magnet and passive structure in that the force arising is a function of the unknown path followed by the halo current in the conducting structure. The poloidal path of the halo current can vary in toroidal direction and, furthermore, eddy currents are believed to contribute to the global force balance.

A summary of the study of the onset of asymmetry of the loads on VV and in-vessel components and the models used to describe it is reported in [20].

Some guideline on how to apply the asymmetric loads on the VV and magnets is described in Appendix I.

7.3.6 Direction of VDE movement and effect on halo current

Although, in a pure loss of vertical position control of the plasma, the probabilities of upward or downward movement of the plasma are predicted to be about equal, the consequences may be calculated to be different as a consequence of the distinct quadrupolar field which exists on the upper and the lower parts of the vacuum chamber. For this reason the peak value of *Ihalo*TPF/Ip* may be different (typically smaller) for an upward VDE versus a downward VDE where the quadrupolar field is larger and therefore the resulting loads are expected also to be greater. The upward VDE design value of *Ihalo*TPF/Ip* should therefore be calculated based on the scaling obtained from analytical results which will indicate the absolute maximum value of halo currents in an upward VDE compared with a downward VDE.

Based on present estimate the upward VDEs generate halo currents loads that are 20% smaller than in downward VDEs.

7.3.7 Load combination of vertical and horizontal forces

From the analysis of experimental data on present running fusion devises it is observed that the maximum horizontal and vertical forces never occur simultaneously. It is recommended to consider two representative combinations:

- Largest vertical force with half of the maximum sideway force,
- Largest horizontal force with half of the maximum vertical force.

These combinations shall be used for the design of the supporting systems of the vessel and the TF magnet supports. The majority of the horizontal forces are expected to occur on the TF coils. However, some sideways forces can be expected on the individual CS and PF coils. Quantified values are not yet available and will be defined in the magnet load specification document.

7.4 Magnet fast discharge

The discharge times of the various magnet systems are a result of design choices and are summarised in the magnet DDD11-1.

In a MFD II to avoid that the induced currents and the electromagnetic loads on the VV and In-vessel components exceed acceptable values, the equivalent time constant of the current decay of the TFC shall not be smaller than 11 s as specified in PR [1].

7.5 Vacuum Vessel ICE

As a consequence of the presence of the pressure suppression system, all in-vessel ICEs type will lead to a pressure in the vessel that never exceeds 0.2MPa. Scenarios and pressure values are reported in [24][25].

The next table summarises the conditions for the three types of events

Table 7-18: Defined types of VV ICEs

	Ref. Event [23]	Cat.	Number of events	Type of break	Break area	Pressure in plasma chamber
VV ICEII	V1	II	15	Double ended break of 1-10 first wall cooling pipes	1.57E-3 m²	106 kPa
VV ICEIII	-	III	1	Double ended break of: Single blanket module branch pipe, or 10-100 first wall pipes	4.0E-3 m²	150 kPa
VV ICEIV	V2	IV	-	Multiple double ended break of >100 first wall cooling pipes	20E-3 m²	200 kPa

7.5.1 VV ICE-II

The worst postulated event is initiated by a failure 1 or 10 first wall cooling pipes, resulting in water ingress into the vacuum vessel, which causes a plasma disruption. The vacuum vessel is pressurized by water/steam injected through the break. The VVPSS bleed lines open at 94 kPa in the VV. The pressure suppression system is effective in keeping the pressure in the plasma chamber at the level <106 kPa. The number of occurrence of this event for component design purpose is 15.

7.5.2 VV ICE-III

For this type of event the worst conditions correspond to a discharge from multiple coolant channels affecting 1 PHTS loop of the First Wall cooling system (e.g. caused by runaway electron initiated damage) or 1-2 coolant channels of divertor and other in-vessel components. The absolute pressure in the VV never exceeds 150 kPa. This event is expected to occur no more than once in the machine life.

7.5.3 VV ICE-IV

The worst VV ICE event corresponds to a multiple break of FW cooling tubes with total break size of 0.02 m^2, resulting in the three FW/BLK cooling loops spilling water inside the VV. The analysis of this event shows that the VVPSS functions efficiently to control the VV pressure transient, limiting the VV peak pressure to 150.1 kPa, which rapidly decreases after reaching this maximum and which is below the VV safety assessment maximum value of 200 kPa. The analysis also shows that the VVPSS is able to control the VV overpressure if the in-vessel coolant leak occurs during baking operation, limiting the VV peak absolute pressure to 151 kPa. In this case, the results also show a sharp VV pressure decrease after the opening of the VVPSS rupture disks.

7.6 Cryostat ICE

Two different types of ingresses into the cryostat are considered [24]:

- Water ingress, cat V (beyond design basis)
- Helium ingress, cat II, III, and IV depending on the amount of leaking He.

Water ingress in the cryostat is an event that is considered beyond design basis as all water pipes inside the cryostat have guard pipes that collect the water from any possible leak. In case of water ingress, anyway, most of the steam would freeze onto the cold magnet surfaces and form ice. As a consequence the cryostat internal pressure would increase only moderately.

In case of He ingress the helium will remain in gaseous state and the cryostat internal pressure will increase more significantly. The He gas causes conduction heat transfer between the cryostat (≈3000t, RT) and the magnets (≈10000t, 4K), which causes a cool-down of the cryostat. Based on conservative estimate, the temperature of the cryostat can decrease to a minimum temperature of 200 - 240 K. This creates contraction of the pedestal ring and cryostat main cylinder in the order of 15 - 22 mm. Unless more detailed and refined calculation are performed, as a measure of conservatism, the pedestal ring columns shall be designed to accommodate a radial thermal contraction of 25 mm (36 mm at the outer skirt). In case of a small He leak (category II) it is assumed that a fast discharge can be avoided, larger He leaks (category III and IV) can however trigger a fast discharge of the magnet system. The next tables summarises the different types of Cr ICEs.

Table 7-19: Defined types of Cr ICEs

	Cat.	Ingress of	Ref. Event	Number of events	Break size	Max. pressure in cryostat
Cr ICEII	II	He		1	0.5 tons (10% of total inventory)	30 kPa
Cr ICEIII	III	He	C3	1	2.6 tons (50% of total inventory)	140 kPa
Cr ICEIV	IV	He		-	4.0 tons (77% of total inventory)	200 kPa
Cr ICE Water	V	Water	C2	1	Single blanket module pipe – ID=66 mm	100 kPa

The simultaneous ingress of water and helium is considered a hypothetical accidental event beyond design basis.

Scenarios and pressure values are reported in [24][25].

7.7 Loss of vacuum inside the VV

In this event the air ingress through one horizontal VV/cryostat penetration line causes pressurization in the VV. The calculated pressure in the VV never exceeds atmospheric pressure.

This event is defined here as VV LOVAIII and corresponds to the ITER Reference Event V3 [24]. It is considered a category III condition

Scenarios and pressure values are reported in [24].

7.8 Loss of vacuum inside the Cryostat

Cryostat leaks are investigated as accidents. A maximum leakage is postulated to be 0.2 m^2 that is estimated on the basis of a bellow failure.

A postulated cryostat air ingress event was analyzed in order to evaluate the depressurization of the cryostat and gallery, temperature inside both volumes, and the magnet temperature, as well as the weight of the air-ice condensed on the coil surfaces. Pressure in the cryostat and in the gallery never exceeds 110 kPa absolute pressure.

The air flowing into the cryostat condenses on the cryogenic surfaces of the superconducting coils, and air-ice is formed on them. The weight of the air-ice mass is negligible compared with that of the coils. It is not expected that the air-ice formed on the coils poses any threat to the structural integrity of the coils.

This event is defined here as Cr LOVAIII and corresponds to the ITER Reference Event C1 [24]. It is considered a category III condition and is assumed to occur no more than once in the life of the machine.

Scenarios and pressure values are reported in [24].

7.9 Loss of Coolant Accident (LOCA) outside the Cryostat

Table 7-20 reports a summary of the LOCA outside events listed in section 6.9.

Table 7-20: Defined types of Ex-cryostat LOCA events

Ex-vessel LOCA	Cat.	Ref. Event	Type of break	Max. pressure	Temperatures
LOCA in galleries	III	X4	VV cooling pipe break (baking), ID=406 mm	Galleries: 106 kPa Vault: 102 kPa	Galleries atmosphere: ≤90°C VV: ≤200°C In-vessel components: ≤270°C
In port cell - LOCA_PC	III	X8	Blanket cooling pipe, ID=66 mm (plasma operation)	Port cell: 120 kPa VV chamber: 94.3 kPa Port duct: 120 kPa Vault: 100 kPa	Port cell atmosphere <120 °C Vault atmosphere: ≤50°C Galleries atmosphere: ≤40°C VV: 100°C
			Blanket cooling pipe, ID=27 mm (baking)	Port cell: 160 kPa VV chamber: 0 kPa Port duct: 150 kPa Vault: 102 kPa	Port cell atmosphere: ≤120°C Vault atmosphere: ≤50°C Galleries atmosphere: ≤40°C VV: 200°C
In NB cell - LOCA_NB	III	Bounding case (in terms of safety) for this event is a cooling pipe break in a port cell.			
In vault - LOCA_Vault	IV	X5	Divertor cooling pipe break - 467 mm² In-vessel Divertor cooling pipe break - 0.2 m² (plasma operation)	VV chamber: 151 kPa Vault: 120 kPa	Vault atmosphere: ≤140°C In-vessel components: ≤250°C
			Divertor cooling pipe break - 467 mm² (baking)	Vault: 191 kPa	Vault atmosphere: ≤140°C In-vessel components: ≤250°C

7.10 Loss of Forced Flow Accident

As described in 6.10 there is no Loss of Forced Flow Accident to be considered for the design of the VV, as this event is classified in category V.

A category III event is considered for the Loss of Forced Flow in the blanket and divertor cooling circuits. As the amount of residual heat to be removed is limited, no large temperature excursion is expected in these events.

Table 7-21 reports a summary of the postulated LOFA.

Table 7-21: Defined types of LOFA events for in-vessel components

	Cat.	Number of events	Cooling circuit	Temperature
IVC LOFAIII	III	1	One circuit of first wall/blanket or divertor	VV temperature: 100°C

7.11 Helium Ingress in Galleries

Table 7-22: Helium Ingress in Galleries

	Cat.	Ingress of	Number of events	Event parameters	Max. pressure in galleries
Helium Ingress in Galleries	III	Helium	1	He spilled: 2.6 tons	118 kPa

8 References

[1] Project Requirements (PR) (ITER_D_27ZRW8).

[2] Heat and Nuclear Load Specifications (ITER_D_2LULDH)

[3] Abstract of ITER Seismic Safety approach (ITER_D_2DRVPE)

[4] Règles fondamentales de sûreté relatives aux installations nucléaires de base – RFS n°2001-01- or RFS 2001-01 Fundamental Safety Rule - determination of seismic risk for basic nuclear installation (ITER_D_2DUKSX).

[5] A Probabilistic Approach to Seismic Hazard in Metropolitan France (ITER_D_22JLSU)

[6] 60SI00-JCB-PKJ-01 ITER Site Investigation Interpretative Report (ITER_D_2M3XEC)

[7] Données sismiques pour les inb de surface du site de cadarache (ITER_D_ 2EPRCQ)

[8] TRANSLATION OF NUCLEAR SAFETY AUTHORITY GUIDELINES ASN/GUIDE/2/01: TAKING SEISMIC RISK INTO CONSIDERATION FOR NUCLEAR FACILITY CIVIL WORKS DESIGN (ITER_25EUYG)

[9] Not used

[10] U.S. Nuclear Regulatory Commission - REGULATORY GUIDE 1.92Combining modal responses and spatial components in seismic response analysis – Washington, DC 20555-0001 – July 2006

[11] U.S. Nuclear Regulatory Commission - REGULATORY GUIDE 1.61-DAMPING VALUES FOR SEISMIC DESIGN OF NUCLEAR POWER PLANTS - Washington, DC 20555-0001 - March 2007.

[12] Loarte, A. et al., in Fusion Energy 2004 (Proc. 20th Int. Conf. Vilamoura, 2004) (Vienna: IAEA) CD-ROM file IT/P3-34

[13] Loarte, A. et al., in Fusion Energy 2006 (Proc. 21st Int. Conf. Chengdu, 2006) (Vienna: IAEA) CD-ROM file IT/P1-14

[14] Wesley, J., et al., in Fusion Energy 2006 (Proc. 21st Int. Conf. Chengdu, 2006) (Vienna: IAEA) CD-ROM file IT/P1-2

[15] Hender, T. et al., 34th EPS, Warsaw (2007).

[16] Wesley, J. 11th ITPA MHD Topical Group Meeting, Feb 25-29, 2008, Naka

[17] Not used

[18] ITER Physics Basis, Nucl. Fusion 39 (1999) 2137.

[19] Progress of ITER Physics Basis, Nucl. Fusion 47 (2007) S175.

[20] Asymmetric Forces on the ITER Vacuum Vessel due to the Sink and Source Model (ITER_D_2DJ5AA)

[21] Not used

[22] ITER INB Preliminary Safety Report (English version) (ITER_D_3ZR2NC V3.0)

[23] Accident Analysis Report (AAR) Volume I - Event Identification and Selection (ITER_D_2DPVGT v1.4)

[24] Accident Analysis Report (AAR) Volume II - Reference Event Analysis (ITER_D_2DJFX3 v4.10)

[25] Accident Analysis Report (AAR) Volume III - Hypothetical Event Analysis (ITER_D_2E2XAM v4.9)

[26] 7.3.3 Simulation results by DINA – Root in IDM: / IDM Root / Project Integration, Administration & Services / 1.9 Plasma Physics / 7. Plasma Control / 7.3 Disruption Control / 7.3.3 Simulation results by DINA

[27] Design Seismic Floor Response Spectra in the Tokamak Complex (SVBRJZ)

[28] Preliminary Design - Hot Cell Facility Building - PBS 62.21 - Response Spectra (42GVVS)

[29] Preliminary Design - Rad Waste Building - PBS 62.23 - Response Spectra (42J38D)

[30] Preliminary Design - Personnel Access Control Building Floor - PBS 62.24 - Response Spectra (42K59H)

[31] Safety Important Functions and Components Classification Criteria and Methodology (ITER_D_347SF3).

[32] ITER Structural Design Code for Buildings (I-SDCB) - Part1: Design Criteria (ITER_D_283B24)

[33] Not used

[34] Not used

[35] DINA_halo_balance_in_blanket (2V2CKX)

[36] Re-examinations of maximum halo current flowing to BM#1 (6SNLQS)

[37] European Norms - EN 1998 Eurocode 8 Earthquake

[38] Order of 22 October 2010 relating to classification and to paraseismic construction regulations applicable to buildings of the class referred to as “of normal risk” - EN (66MEA7)

[39] Loss of Water and Cryogenic Coolant into the Gallery, ITER_D_2ABK4S

[40] Database on ‘slow+fast’ CQ waveform and proposal for its specification to ITER scenario (6TB9ML)

[41] Not used

[42] Global Tokamak Seismic Analysis Report (33W3P4)

[43] Eurocode 8: Design provisions of earthquake resistance of structures, Part 4: Silos, tanks and pipelines. European Committee for Standardization, Brussels, 1998.

[44] Seismic Analysis of Safety-related Nuclear Structures, ASCE 4-98, American Society of Mechanical Engineers

[45] ASME Boiler and Pressure Vessel Code, Section III, Div.1 - Rules for Construction of Nuclear Facility Components, NMA Appendix N – Dynamic Analysis Methods, (2001), - pp. 330-399

[46] Not used

[47] Codes and Standards for ITER Mechanical Components (ITER_D_25EW4K)

Appendix A: Summary of the design specification data for plasma disruptions and VDEs.

Table A-1.1: Main Specifications for disruptions classified based on the current quench speed

Load case	Units	MD I	MD II	MD III	MD IV fast	MD IV Slow_fast
Load category	-	I - Normal	II - Likely	III - Unlikely	IV Extremely unlikely	
Number of events		2600	400	-	-	-
TPF*Ih/Ip	-	0.15	0.15	0.15	0.15	(*)
Typical direction of plasma movement		Inward and Upward/Downward				
Current quench duration (if Linear decay)	ms	50	36	36	26	(**)
Current quench duration (if Exp decay)	ms	22	16	16	11.3	NA

(*) As a full characterisation of the slow_fast event is not completed, it can be assumed conservatively that the same halo current as in Slow VDE III are applied for upper and lower vertical movements of the plasma.

(**) Plasma current decay is initially slow, later dIp/dt is the same as MD III fast in linear plasma current decay.

Table A-1.2: Main Specifications for disruptions classified based on the thermal quench speed (*)

Load case	Units	MD I	MD II	MD III (IV)
Load category	-	I - Normal	II - Likely	III (IV)
Number of events		2600	400	-
Max. Thermal energy at beginning of TQ	GJ	0.2	0.35	0.35
Min. Energy quench time	ms	3	1	0.5

(*) Parameters related to plasma thermal quench are also defined in [2].

Table A-2a: Main Specifications for VDEs II

Load case	Units	VDE II Slow		VDE II Fast	
Direction of initial drift		Up	Down	Up	Down
Load category		II - Likely Event			
Number of events		300			
Max TPF*Ihalo/Ip		0.34	0.42	0.20	0.25
Max Ihalo/Ip		0.24	0.30	0.15	0.18
Edge q at start of thermal quench		1.5~2.5			
Minimum edge q during current quench		~1			
Typical current quench duration	ms	50 ~ 100		See MD II	
Horizontal Force on VV/magnets	MN	27	12	16	7
Vertical Force on VV/magnets	MN	48	-60	29	-36

Table A-2b: Main Specifications for VDEs III and IV

Load case	Units	VDE III Slow		VDE III Fast		VDE IV Slow_Fast	
Direction of initial drift		Up	Down	Up	Down	Up	Down
Load category		III - Unlikely Event				IV - Unlikely Event	
Number of events		N/A				N/A	
Max TPF*Ihalo/Ip		0.60	0.75	0.36	0.45	0.60	0.75
Max Ihalo/Ip		0.44	0.54	0.26	0.33	0.44	0.54
Edge q at start of thermal quench		~1.5				~1.5	
Minimum edge q during current quench		~1				~1	
Typical current quench duration	ms	> 200		See MD III		(**)	
Horizontal Force on VV/magnets	MN	48	22	29	13	48	22
Vertical Force on VV/magnets	MN	86	-108	52	-65	86	-108

(**) Plasma current decay is initially slow, later dIp/dt is the same as MD III fast

No runaway electrons are expected for all VDE cases.

Appendix B: List of load cases and case combinations to help the system load specification document preparation

The following tables are templates for the preparation of the full list of load cases and load case combinations that shall be used in the development of the load specification for each system or component.

The list is intended to define all possible loads, but for many systems some of the loads and load combinations are negligible or are enveloped by other combinations. This has to be assessed on a case-by-case basis.

The operating conditions (second columns of the tables) shall include the conditions of the system that are possible to be present at the time the initiating triggering event occurs. These conditions depend on the status of the components or the plants during the combination event (operation, baking, maintenance, superconducting magnet energised, vacuum pumping, etc.). These include, but not limited to:

- Dead weight of the component and all attached structures (DW)
- Pressure of coolant (CP), operating pressure or vacuum loads, etc.
- Temperature values and thermal loads (TH)
- Assembly and preloads
- Service loads

The tables define an initiating event. This is the event that is considered the major cause of triggering other events or loads. The definition of the triggering event is important for the definition of the time sequence of the event and the evolution of the associated loads. This is important for the definition on how maxima values of load are combined.

The last columns include some recommendations on how certain event combinations can be excluded for being analysed in details as the load associated are probably enveloped by other case combinations. It indicates also if maximum associated loads are not concomitant in time. It is anyway recommended that this is verified in details for each system under investigation and that the reason for exclusion of a load case combination to be provided.

In case of seismic events combined with other accident conditions (i.e. Cr ICEs) the loads are conservatively considered concomitant in time to account for seismic aftershock (a second seismic shock that follows a previous seismic event responsible of the accident conditions)

Table B-1: List of events and event load combinations in category I and II (8)

	Operating conditions (1),(4)	Initiating event	Concatenated events	Cat	# of events (2), (3)	Comment (9)
I.1	DW,CP,TH..			I		
I.2	DW,CP,TH..	**MD I**		I	2600	Enveloped by I.4
I.3	DW,CP,TH..	**MFD I**		I	500	Enveloped by I.4
I.4	DW,CP,TH..	**MFD I**	MD I	I	500	
II.1	DW,CP,TH..	**MD II**		II	400	Enveloped by II.4 except for failure due to cyclic loads
II.1a	DW,CP,TH..	**MD II**	VV ICE II	II	15	
II.2	DW,CP,TH..	**VDE II**		II	300	Enveloped by II.4a except for failure due to cyclic loads
II.2a	DW,CP,TH..	**VDE II**	VV ICE II	II	15	
II.3	DW,CP,TH..	**MFD II**		II	50	Enveloped by II.5
II.4	DW,CP,TH..	**MFD I**	MD II	II	50	
II.4a	DW,CP,TH..	**MFD I**	VDE II	II	50	
II.5	DW,CP,TH..	**MFD II**	MD I	II	50	
II.6	DW,CP,TH..	**VV ICE II**		II	15	Enveloped by II.7
II.7	DW,CP,TH..	**VV ICE II**	MD I or II	II	15	Maximum load values are not concomitant
II.8	DW,CP,TH..	**Cr ICE II**		II	15	Enveloped by II.9
II.9	DW,CP,TH..	**Cr ICE II**	MFD I or II	II	15	Maximum load values are not concomitant
II.10	DW,CP,TH..	**SL-1**		II	1 (7)	Enveloped by II.11 and II.12
II.11	DW,CP,TH..	**SL-1**	MD 1	II	1 (7)	
II.12	DW,CP,TH..	**SL-1**	MFD I or II	II	1 (7)	
II.13	DW,CP,TH..	**SL-1**	MD I +MFD I or II	II	1 (7)	

For explanation notes see table B-4.

Table B-2: List of events and event load combinations in category III (2), (5),(8)

	Operating conditions (1),(4)	Initiating event	Concatenated events	Cat	Comment (9)
III.1	DW,CP,TH..	**MD III**		III	
III.2	DW,CP,TH..	**VDE III**		III	
III.3	DW,CP,TH..	**MD II**	VV ICE III	III	Maximum load values are not concomitant
III.4	DW,CP,TH..	**VDE II**	VV ICE III	III	Maximum load values are not concomitant
III.4a	DW,CP,TH..	**MD III**	VV ICE II or III	III	Maximum load values are not concomitant
III.4b	DW,CP,TH..	**VDE III**	VV ICE II or III	III	Maximum load values are not concomitant
III.4c	DW,CP,TH..	**VDE III**	MFD I	III	Maximum load values are not concomitant
III.5	DW,CP,TH..	**MFD II**	Cr LOVA III	III	
III.6	DW,CP,TH..	**MFD II**	MD II	III	Enveloped by III.23a
III.7	DW,CP,TH..	**MFD II**	VDE II	III	Enveloped by III.24a
III.8	DW,CP,TH..	**VV ICE III**		III	Enveloped by III.9
III.8a	DW,CP,TH..	**VV ICE III**	MD I	III	Enveloped by III.9.
III.8b	DW,CP,TH..	**VV ICE III**	MD II	III	Enveloped by III.9.
III.9	DW,CP,TH..	**VV ICE III**	MD III	III	
III.10	DW,CP,TH..	**VV ICE II**	MD III	III	
III.11	DW,CP,TH..	**VV LOCA**		III	
III.12	DW,CP,TH..	**VV LOVA III**		III	Enveloped by III.13
III.13	DW,CP,TH..	**VV LOVA III**	MD III	III	
III.14	DW,CP,TH..	**IVC LOFA III**		III	
III.15	DW,CP,TH..	**Cr ICE III**		III	Enveloped by III.28
III.16	DW,CP,TH..	**Cr ICE III**	MFD I or II	III	Enveloped by III.28
III.17	DW,CP,TH..	**Cr LOVA III**		III	Enveloped by III.18
III.18	DW,CP,TH..	**Cr LOVA III**	MFD I or II	III	
III.19	DW,CP,TH..	**LOCA Galleries III**		III	
III.20	DW,CP,TH..	**LOCA PC III**		III	

III.21	DW,CP,TH..	**LOCA NB III**		III	
III.22	DW,CP,TH..	**Helium leak in Galleries**		III	Enveloped by III.27
III.23	DW,CP,TH..	**SL-1**	MD II	III	Enveloped by III.23a
III.23a	DW,CP,TH..	**SL-1**	MFD II + MD II	III	
III.24	DW,CP,TH..	**SL-1**	VDE II	III	Enveloped by III.24a
III.24a	DW,CP,TH..	**SL-1**	MFD II + VDE II	III	
III.25	DW,CP,TH..	**SMHV**		III	Enveloped by III.27 and III.28
III.26	DW,CP,TH..	**SMHV**	Cr ICE III	III	
III.27	DW,CP,TH..	**SMHV**	Helium leak in galleries	III	
III.28	DW,CP,TH..	**SMHV**	Cr ICE III + MFD I or II	III	

For explanation notes see table B-4

Table B-3: List of events and event load combinations in category IV (2),(6),(8)

	Operating conditions (1),(4)	Initiating event	Other events	Cat	Comment (9)
IV.1	DW,CP,TH..	**MD IV**		IV	Enveloped by IV.5
IV.2	DW,CP,TH..	**VDE IV**		IV	Enveloped by IV.5a
IV.3	DW,CP,TH..	**MD III**	VV ICE IV	IV	Enveloped by IV.5. Maximum load values are not concomitant
IV.4	DW,CP,TH..	**VDE III**	VV ICE IV	IV	Enveloped by IV.5a Maximum load values are not concomitant
IV.5	DW,CP,TH..	**MD IV**	VV ICE III or IV	IV	Maximum load values are not concomitant
IV.5a	DW,CP,TH..	**VDE IV**	VV ICE III or IV	IV	Maximum load values are not concomitant
IV.5b	DW,CP,TH..	**MD III**	MFD I	IV	Maximum load values are not concomitant
IV.6	DW,CP,TH..	**VV ICE IV**		IV	Enveloped by IV.7
IV.7	DW,CP,TH..	**VV ICE IV**	MD I or II or III	IV	
IV.8	DW,CP,TH..	**VV ICE II**	MD III	IV	Enveloped by IV.7
IV.9	DW,CP,TH..	**Cr ICE IV**	MFD I or II	IV	
IV.10	DW,CP,TH..	**SL-2**		IV	Enveloped by IV.12, IV.13, IV.14
IV.11	DW,CP,TH..	**SL-1**	MD III	IV	
IV.12	DW,CP,TH..	**SL-2**	Cr ICE III	IV	
IV.13	DW,CP,TH..	**SL-2**	Int Fire	IV	
IV.13.1	DW,CP,TH..	**SL-2**	LOOP	IV	
IV.14	DW,CP,TH..	**SL-2**	Helium leak in Galleries	IV	
IV.15	DW,CP,TH..	**SMHV**	Int Fire	IV	Enveloped by IV.13
IV.16	DW,CP,TH..	**LOCA PC III**	VV ICE II	IV	
IV.17	DW,CP,TH..	**LOCA in VAULT**		IV	

For explanation notes see table B-4.

Table B-4: Explanation notes for tables B-1, B-2, B-3

Note	
(1)	Operation conditions: This includes all load conditions that are present at the time the single events or event combinations occur (examples: dead weight - DW, component coolant pressure - CP, Thermal loads – TH, etc.) that are at least probable to be present in the event combination. If the probability of these additional conditions to be present is low, considerations or justifications have to be made for the definition of the load category of the combination.
(2)	Unless a detail dynamic analysis is performed and the number of cycles per event is directly calculated, it is recommended to assume for each seismic event 10 equivalent maximum stress cycles whenever a fatigue or a cyclic load analysis is required. For disruptions and VDEs the number of equivalent cycles per event has to be determined based on the dynamic response of each single component.
(3)	This column reports the maximum value of events. This number is reduced if this event is combined with other events (i.e. MDI + MFD, MDII + ICE II, VDE II + ICE II). The reduction corresponds to the number of events assumed in the additional combinations.
(4)	In combination with seismic events the system or component shall be considered with the plan in the status (examples: shut-down, superconducting magnet energised, baking, plasma operation, etc.) that is considered more severe. In case the more severe status is not clearly identifiable or justifiable more status shall be considered.
(5)	Category III events and combinations shall be assumed to occur once in the machine life unless otherwise specified.
(6)	The number of events is not specified as these events have very low probability of occurrence. For these events a failure mode that is caused by the repetitive application of the load (fatigue, ratchetting) is not required.
(7)	As the SL-1 level is defined on a seismic event with a return period of more than 100 years it is expected to occur only once in the machine life. If required by investment protections it shall be assumed to occur a maximum number of 5 times.
(8)	In the stress report of the components, the load combination which is most critical for each specific area of that component shall be clearly identified and the details of the load case considered (e.g. directions, peak values etc.) shall be explicitly reported
(9)	This column include some recommendations on how certain event combinations can be excluded for being analysed in details as the load associated are probably enveloped by other case combinations. It indicates also if maximum associated loads are not concomitant in time. It is anyway recommended that this is verified in details for each system under investigation and that the reason for exclusion of a load case combination to be provided.

The following additional accidental events affect mainly the design of the nuclear building. They do not need to be combined with electromagnetic transient and seismic events and are specified in the building load specification documents (600000-CCS-DA0-01 Load Specifications for Buildings with Safety Requirements (ITER_D_2ERTXQ),

Table B-5: Additional accidental conditions for the nuclear building design

	Initiating event	Other events	Cat
B.IV.1	**LOCA Vault IV (only component not building)**		IV
B.IV.2	**Internal explosion**	Internal fire	IV
B.IV.3	**Internal fire**	internal flooding	IV
B.IV.4	**LOCA**	Internal flooding	IV
B.IV.5	**Air crash**	external fire	IV
B.IV.6	**Water table**	external flooding	IV
B.IV.7	**External explosion**	External fire	IV
B.IV. 8	**Accidental temperature**	External fire	IV
B.IV.9	**Internal explosion**	Load drop	IV
B.IV.10	**External fire**	External explosion	IV
B.IV.11	**Internal explosion**	Internal flooding	IV
B.IV.12	**Internal fire**	Internal explosion	IV
B.IV.13	**Damaged equipment**	Internal flooding	IV

Table B-6: Load combinations in category V to be considered for the design and verification of the second safety confinement barrier. (*)

	Event combination	Category
B.V.1	**MFD II** + VDE IV	V
B.V.2	**Cryostat air ingress** + MFD II + VDE II	V
B.V.3	**VDE IV** + VV ICE IV	V
B.V.4	**Cr ICE IV** + MFD II + VDE II	V
B.V.5	**VDE IV** + MFD I	V
B.V.6	**SL-2** + Cr ICE IV (from Magnets and Thermal Shield) + ICE III in gallery + MFD II + VDE II	V
B.V.7	**Cr ICE V** (water leak inside the cryostat)	V

(*) items in bold represent the initiating event

Appendix I: Application of asymmetric loads onto structural models in asymmetric VDEs

The asymmetric loads on the tokamak components can be generated by:

a) asymmetric poloidal halo currents in the passive structures;
b) asymmetry toroidal current in the structures surrounding the plasma which is associated with asymmetric plasma toroidal currents[6]

Available codes to perform plasma simulation in transient events allow only 2D axi-symmetric simulations. Lacking a complete 3D MHD computer simulation of this phenomenon with model of plasma and surrounding passive structures, a simpler approach to the problem is to calculate the horizontal net loads on a plasma 'distorted' by helical instability.

a) Asymmetric poloidal halo current

Loads asymmetries can be taken into account by the introduction of the toroidal peaking factor (TPF), which gives the ratio of peak halo current density to average halo current density.

The major contribution to the net horizontal force on VV, magnets and in-vessel components is considered due to a non-uniform halo current. Eddy current in the plasma surrounding structures due to a plasma kink can also contribute to provide non-asymmetric loads.

Having then fixed both halo peaking factor and net horizontal force, lacking a fully consistent 3D model, to simplify the structural analysis of the tokamak components, in case of asymmetric VDEs, the following assumptions and procedure can be adopted to evaluate halo and eddy currents loads once a 2D self consistent calculation has been performed:

1. The halo current path in the passive structure is assumed constant in the toroidal direction;
2. The halo current amplitude is varied around the toroidal direction with a cosinusoidal pattern, and having a peaking factor as specified;
3. Eddy current loads are also modulated (non uniform) around the torus.

The plasma simulation code calculates the total load P_{tot} in a plasma VDE due to the total halo current I_{halo}. Loads asymmetries can be taken into account by the introduction of the toroidal peaking factor (TPF), which gives the ratio of peak halo current density to average halo current density.

Loads due to the poloidal halo current I_{halo} for TPF≤2 is applied depending on the toroidal angle ψ as:

$$P(\psi)/_{rad} = [\cos(\psi) \cdot (TPF - 1) + 1] \cdot P_{tot}/_{rad}$$

In case of TPF>2 a local concentration of halo current load has to be considered. It has to be assumed that the peak poloidal halo current density is constant, independently of the TPF.

[6] This phenomenology has been observed at JET when the plasma was in kink mode

b) Asymmetry toroidal current in the structures surrounding the plasma associated with asymmetric plasma toroidal current

This asymmetric halo current is different from I_{halo}, which is discussed in the previous chapter. This asymmetric current layout is related to the asymmetry of the plasma toroidal current, which may occur during VDEs. The estimate of the sideways force is based on the required current continuity in toroidal direction, which imposes that the asymmetry of the plasma toroidal current is compensated by an asymmetric toroidal halo current ΔI_p in the VV. The ΔI_p current is assumed equal to 10% of the pre-disruption plasma current. Detailed experimental database for the asymmetry toroidal current is summarized in [A1].

The definition of this asymmetric load is derived from experimental observation of JET data. Ref [20] reports the calculation of the asymmetric loads on the ITER VV extrapolated from the experimental measurements. An equal opposite total set of forces and moments has to be applied to the magnet structures as the total net forces and moment applied to the full tokamak machine has to be zero. It has to be noted that, due to the different natural frequency of VV and magnet structures, the reaction forces on their support is not zero due to dynamic nature of the load and reaction forces.

In JET experiments, a clear phase relation between toroidal asymmetry current and poloidal halo current asymmetry has been observed [A1]. From this observation, direction of horizontal force and the toroidal location of largest poloidal halo current (and thus largest vertical force) can be identified as shown in Fig. A-1.

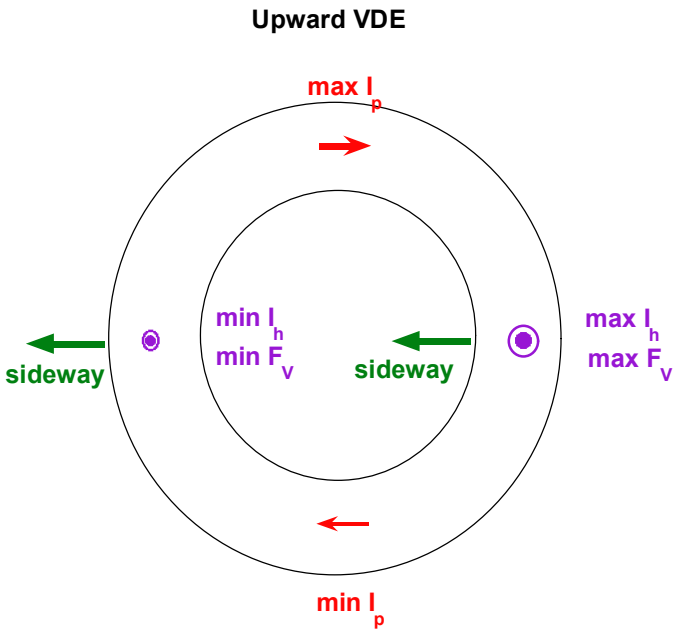

Figure A-1 Phase relation between max/min toroidal plasma current, max/min poloidal halo current, direction of horizontal (sideway) force and maximum vertical (upward) force for upward VDE case viewed from top.

Both plasma current and toroidal field are in clock wise. Note that toroidal current on the vessel is minimum (opposite direction to plasma current) when toroidal plasma current is maximum.

This observation is the basis for the empirical sink & source model developed by JET group [A2] and employed for the assessment of ITER case in [A3].

References

[A1] T. Hender et al., ITPA MHD topical Group, WG-6 final report (2011).

[A2] V. Riccardo et al., Nuclear Fusion 40 (2000) 1805-1810.

[A3] Asymmetric Forces on the ITER Vacuum Vessel due to the Sink and Source Model (ITER_D_2DJ5AA).

Appendix II: Damping values for structural simulation of the tokamak components in plasma transient events

Plasma transient events (namely plasma disruptions and VDEs) induce loads that are generally of limited time duration and vary in a time range that is comparable to the natural periods of the structures. For this reason, the dynamic effects (including structural damping) need to be taken into account.

The energy of the vibrating systems may be dissipated by

a) Energy absorber placed at specific location
b) Mechanism of energy dissipation distributed into the structure

The first mechanism is simulated in structural dynamic analysis model by concentrated damping systems. Damping values shall be calculated and/or demonstrated by analyses or test.

The second mechanism is generally provided by small material plasticity and friction at mechanical connections that are distributed in the structures. As analysis models are generally linear, for analysis convenience this damping is generally assumed to be viscous in nature by the definition of a general structural damping value that is defined as proportional of the critical damping. As plasticity and frictions are more relevant as stress in material and at joints is more severe, and as allowable and calculated stress values are generally higher for events in higher categories, the recommended damping value increases for the higher load category grade. Table II-1 reports the value of the recommended structural damping values for the tokamak components for loads in different categories.

Table II-1 – Damping ratios for the tokamak components for dynamic analysis of plasma transient events at different load categories

Load category	Category I and II	Category III	Category IV
Percentage of critical damping	2%	3%	4%

For specific equipment the damping value could be larger than the values reported in table II-1. It is allowed to use different values, provided that they are justified.

It has to be noted anyway that the damping values has not a large effect on the dynamic response to impulse (or short-lasting) loads as those generated by the plasma fast transient events.